Biogeosciences, 21, 2029–2050, 2024
https://doi.org/10.5194/bg-21-2029-2024

Biogeosciences Open Access EGU

Picoplanktonic methane production in eutrophic surface waters

Sandy E. Tenorio[1,2,4] **and Laura Farías**[1,2,3]

[1]Departamento de Oceanografía, Facultad de Ciencias Naturales y Oceanográficas, Universidad de Concepción, Concepción, 4070043, Chile
[2]Centro de Ciencia del Clima y la Resiliencia (CR2), Santiago, Chile
[3]Instituto Milenio en Socio-ecología Costera (SECOS), Santiago, Chile
[4]Programa de Graduados en Oceanografía, Departamento de Oceanografía, Universidad de Concepción, Concepción, 4070043, Chile

Correspondence: Laura Farías (laura.farias@udec.cl)

Received: 3 October 2023 – Discussion started: 9 October 2023
Revised: 27 February 2024 – Accepted: 28 February 2024 – Published: 25 April 2024

Abstract. Over the past decade, extensive research has delved into the methane (CH_4) paradox, which involves aerobic CH_4 production. We present noteworthy observations of CH_4 oversaturation within the surface layer of the central Chile upwelling zone (36° S, 73° W) over two consecutive seasonal cycles (2018–2021). Complementing these observations, CH_4 cycling experiments were conducted, utilizing distinct plankton fractions (encompassing the natural planktonic community, fractions < 150, < 3 and $< 0.2\,\mu m$), in different productivity periods of phytoplanktonic production and composition throughout the year. Our findings underscore the pivotal role of picoplankton ($< 3\,\mu m$) in CH_4 production on the ocean surface, contrasting with the limited contribution of larger microorganisms ($< 150\,\mu m$). Notably, incubations with methylated substrates, such as methylphosphonic acid (MPn) and trimethylamine (TMA), induce heightened CH_4 production within the picoplanktonic fraction. This phenomenon is consistently observed during both upwelling (austral spring–summer) and non-upwelling (winter) seasons, with significance in the latter period, when *Synechococcus sp.* exhibits notably high relative abundance. Long-term microcosm experiments highlight the crucial roles played by heterotrophic bacteria and cyanobacteria in methylotrophic methanogenesis. This process enhances CH_4 production, facilitated by the recycling of dissolved organic carbon (DOC). Picoplankton emerges as a pivotal factor influencing the recycling of methylated substrates, and it is responsible for maintaining CH_4 supersaturation. These findings provide valuable insights into the biogeochemical processes driving CH_4 dynamics, particularly in highly productive upwelling areas.

Key points.

1. Picoplankton plays a crucial role in maintaining CH_4 supersaturation in the surface layer under different oceanographic conditions, influencing its exchange with the atmosphere.
2. Methylated substrates, such as methylphosphonic acid (MPn) and trimethylamine (TMA), notably stimulate CH_4 production through picoplankton-mediated methylotrophic methanogenesis.
3. *Synechococcus sp.*, utilizing the MPn substrate during the non-upwelling season, and picoeukaryotes, utilizing the TMA substrate during the onset of upwelling, could emerge as crucial microorganisms involved in CH_4 generation.

1 Introduction

Methane (CH_4) is a short-lived yet potent greenhouse gas, exhibiting a significantly higher heat-trapping capacity than CO_2 over a century. Its importance lies in its substantial influence on global climate dynamics and the necessity for robust mitigation strategies (IPCC, 2021; Harmsen et al., 2020). The ocean holds considerable amounts of dissolved and hydrate CH_4, rendering its thorough study crucial for precise climate change modeling and comprehending its ecological diversification within oceanic ecosystems (IPCC, 2021; Xu et al., 2022).

The distribution of CH_4 is intricate and influenced by both complex physical (transport) and biogeochemical (production and consumption rates) processes (Reeburgh, 2007). In the open ocean, surface waters generally display slight oversaturation, whereas deeper waters tend toward equilibrium or undersaturation with respect to the atmosphere. However, there is often CH_4 accumulation within the pycnocline (Lamontagne et al., 1973; Cicerone and Oremland, 1988; Holmes et al., 2000). These distribution patterns led to the identification of the CH_4 paradox (see review in Reeburgh, 2007). Early hypotheses have suggested various sources for CH_4 oversaturation in the surface layer, including organic matter respiration within anoxic niches of particulate organic material (Karl and Tilbrook, 1994), within fish (Oremland, 1979) and in zooplankton guts (De Angelis and Lee, 1994). However, these classical methanogenesis pathways remain obscured in the surface and oxic zone of aquatic systems. Subsequent advancements in this field highlighted biochemical processes, such as methylotrophic methanogenesis, now understood as the production of CH_4 from methylated compounds under diverse biogeochemical conditions (Karl et al., 2008; Damm et al., 2010, 2015; Repeta et al., 2016).

Methylated compounds are synthesized or degraded by diverse autotrophic and heterotrophic microorganisms; for example, *Nitrosopumilus maritimus* produces phosphonates like methylphosphonic acid (MPn) (Metcalf et al., 2012), whereas different species of phytoplankton, in turn, contribute to sulfur derivates such as methionine (Lenhart et al., 2016), dimethylsulfoniopropionate (DMSP), dimethyl sulfide (DMS) (Belviso et al., 1990; Stefels and Van Boekel, 1993) and trimethylamines (TMA) (Sun et al., 2019), serving as potential carbon sources for microorganisms and thereby contributing to CH_4 generation via methylotrophic methanogenesis. Furthermore, there is a suggestion that photosynthesis plays a role in direct CH_4 production (Berg et al., 2014; León-Palmero et al., 2020; Klintzsch et al., 2023). Several studies have shown associations between CH_4 anomalies in surface waters and specific phytoplanktonic groups, such as coccolithophores (Lenhart et al., 2016) and cyanobacteria (Bižić et al., 2020). Hence, recognizing phytoplankton in various size fractions as direct links to CH_4 production in diverse marine ecosystems (Bizic, 2021) becomes imperative, especially through pathways involving demethylation from methylated compounds (Damm et al., 2010; Florez-Leiva et al., 2013; Lenhart et al., 2016; Karl et al., 2008; Sun et al., 2011; Repeta et al., 2016).

Coastal upwellings, due to their high productivity, represent an emblematic site for the study of CH_4 production, but the proximity to anoxic sediments and prevalent anaerobic methanogenesis in sediments or in the oxygen minimum zones (OMZs) often obscures the study of CH_4 generation within oxygen-rich surface waters. Indeed, CH_4 profiles predominantly exhibit significant increases towards anoxic sediments (Farías et al., 2021; Ma et al., 2020; Kock et al., 2008). Coastal regions serve as intensive CH_4 sources, facilitating lateral transport to open waters (Borges and Abril, 2012; Upstill-Goddard and Barnes, 2016) and/or the atmosphere due to vertical advection linked to coastal upwelling (Farías et al., 2021; Kock et al., 2008). Current global CH_4 balances exhibit high uncertainly (Saunois et al., 2020; Roth et al., 2022; Lu et al., 2021) and considerable spatial and temporal variability, particularly in coastal environments, where fluxes represent over 40 % of total atmospheric fluxes (Weber et al., 2019; Bange et al., 1994).

Given the upwelling systems are expected to integrate all above-mentioned mechanisms, investigating CH_4 dynamics becomes pivotal. Upwelling processes dynamically transport nutrient-rich water onto continental shelves and the surface, significantly enhancing biological productivity to eutrophic levels. This surge in high microbial productivity, biomass and organic matter decomposition establishes these areas as pivotal hubs for carbon cycling, particularly in CH_4 (Capone and Hutchins, 2013). Indeed, in upwelling systems a large part of the primary production is channeled to dissolved organic carbon (DOC) through the microbial food web and a smaller percentage directly to copepods via the herbivore food chain (Vargas et al., 2007). In addition, coastal areas receive large amounts of DOC from rivers (Bianchi, 2011), and this is also the case of upwelling systems off central Chile (Vargas et al., 2013). These microbial food web and riverine pathways not only transport and remineralize nutrients and DOC but also foster the generation of greenhouse gases like CH_4 (Dinasquet et al., 2018; Sun et al., 2019).

Crucially, specific microbial groups such as *Pelagibacter*, SAR11, considered key players in DOC recycling, have been identified as potential contributors to CH_4 regeneration from diverse C1 compounds (Carpenter et al., 2012; Repeta et al., 2016; Sun et al., 2019). The synergy between autotrophic (e.g., picoeukaryotes, cyanobacteria) and heterotrophic picoplankton ($< 3\,\mu m$) could represent pathways for CH_4 production in coastal regions. Therefore, the main aim of this study is to investigate the dynamics of CH_4 oversaturation within the surface layer of the central Chile upwelling zone using observational and experimental approaches. Among objectives are to discern the contributions of different plankton fractions, particularly picoplankton, and to unravel the involvement of methylated substrates like MPn and TMA in stimulating CH_4 production. Ultimately, this research will provide comprehensive insights into the biogeochemical mechanisms that drive CH_4 dynamics within highly productive upwelling water, emphasizing the role of picoplankton in maintaining CH_4 oversaturation in the surface ocean.

2 Material and methods

2.1 Regional setting

The continental shelf off central Chile undergoes wind-driven coastal upwelling, seasonally controlled by the migration of the South Pacific anticyclone (Strub et al., 1998). This process leads to alongshore equatorward winds during the summer–spring period, producing coastal upwelling (Sobarzo and Djurfeldt, 2004; Sobarzo et al., 2007). The area is influenced by Equatorial Subsurface Water (ESSW), which is nutrient-rich and has low dissolved O_2 levels (less than 44 µM). The ESSW interacts with sediments and serves as a nutrient source during coastal upwelling, delivering low O_2 concentrations and high organic matter content to the bottom water and sediments, fostering anaerobic organic matter mineralization supporting denitrification, sulfate reduction and methanogenesis (Ferderlman et al., 1997; Farías et al., 2004).

2.2 Water collection

Seawater was collected from the upwelling zone of central Chile (36°0.802′ S; 73°07.750′ W) at the University of Concepción's time series station (ST18), situated at a depth of 90 m (Fig. 1). Monthly samplings have been conducted on board the RV *Kay–Kay II* since 2002. Continuous sampling with a CTD-O (conductivity, temperature and depth including oxygen; SBE 19) instrument was performed to obtain temperature, salinity and dissolved oxygen (DO) profiles, whereas seawater samples using 10 L Niskin bottles at various depths (0, 5, 10, 20, 30, 50, 65 and 80 m) were obtained in triplicate for dissolved gas (DO and CH_4), nutrient and chlorophyll-*a* (chl-*a*) analysis. Detailed methodologies can be found in Farías et al. (2021). From March 2019 to June 2020, DOC samples were specifically procured from depths of 5, 20, 50 and 80 m.

To investigate the role of differently sized planktonic communities in CH_4 cycling, seawater was gathered at a depth of 10 m, a depth commonly associated with the chl-*a* peak (Testa et al., 2018). Large zooplankton (150 µm mesh sieve) were excluded using the methodologies outlined by Sieburth et al. (1978). The experimental setup is outlined in Table 1 and includes two negative controls: (1) sterile filtration using a 0.2 µm filter, an often-used method for the removal of microorganisms (Hahn, 2004), and (2) poisoning with the addition of $HgCl_2$ to ensure total inactivation of the few bacterial species which can pass through 0.2 µm filters (Hahn, 2004). The positive control was the natural community (NC) without any filtration.

Another set of experiments enriched with the organic methylated substrates MPn and TMA were performed using only the fractioned picoplanktonic community. To maintain the integrity of the samples, seawater was transported in dark and refrigerated drums placed inside expanded polystyrene boxes surrounded by ice packs to preserve the natural temperature of the seawater (∼ 13 °C) and minimize microbial activity. The average time for transportation to the Marine Station Biology Laboratory at Dichato was approximately 4 h. However, it is important to note that there were delays of 8 to 12 h between arrival at the laboratory and the onset of short- and long-term experiments, respectively. These delays were due to filtering and a short acclimatization process (6 h) required before initiating the experiments, but these procedures were done in a cool room (13 °C).

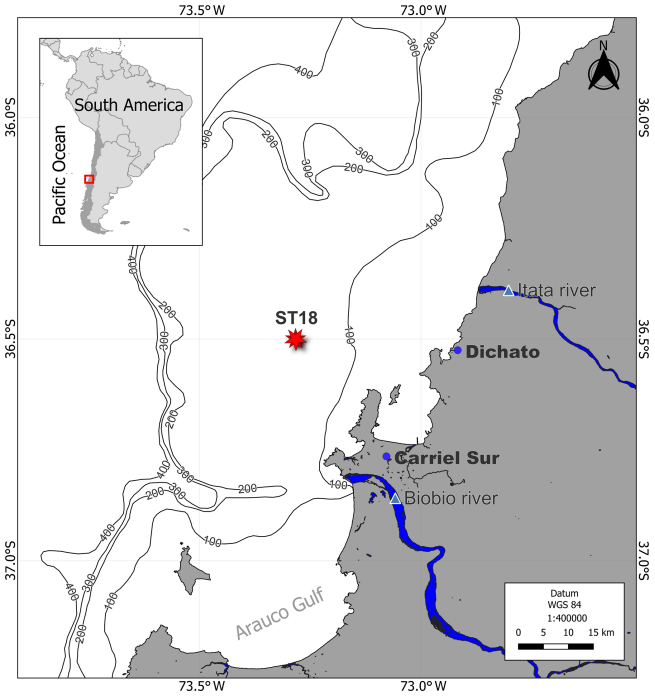

Figure 1. Time series location map (ST18) over the central Chile upwelling platform. The Itata and Biobio rivers, Carriel Sur meteorological station, and town of Dichato are indicated.

This is a time series study, from 2018 until 2021, encompassing CH_4 regeneration in different productivity phases (Table 1) according to Testa et al. (2018). In this regard, two types of experiments described in the following sections will be conducted.

2.3 Short-term experiments of CH_4 cycling from size-fractionated planktonic community enriched with organic substrates

The size fractionation of planktonic communities was conducted through a careful sequential filtration process, where 5 L of seawater was gently passed through a pre-filter of 150 µm nylon, followed by 3 µm Isopore and 0.22 µm Millipore membranes, yielding two fractions: picoplankton (< 3 µm) and femtoplankton (< 0.2 µm) communities; the last one was used as a negative control in some experiments. NC was obtained directly without filtering (Table 1).

Table 1. Summary of the experimental setup of short-term (GC vials) and long-term (microcosms) experiments with different treatments. NC: seawater with the natural plankton (control); $< 3\,\mu m$: picoplankton; $< 0.2\,\mu m$: femtoplankton (control +); $< 0.2\,\mu m + HgCl_2$: femtoplankton with $HgCl_2$ (control +); CC: picoplankton concentrate; and the addition of methylated substrates (MPn: methylphosphonic acid; TMA: trimethylamines). Different phases of the productivity period are as follows: PI – Phase I; PII – Phase II; and PIII – Phase III.

Date	Type of experiment	Setup	Plankton size (µm)	Place	Time (h)	Productivity period
December 2018	GC vials	Plankton fractionation	CN, < 3 and < 0.2	Incubator	24	High (PI)
January 2019	GC vials	Plankton fractionation	CN, < 3 and < 0.2	Incubator	24	High (PI)
March 2019	GC vials	Add: MPn	< 3	Incubator	24	Intermediate (PII)
May 2019	GC vials	Add: MPn and TMA	< 3	Incubator	24	Basal (PIII)
April 2019	Microcosms	Add: MPn and TMA	CN, < 3 and CC	Cold room	~ 60	Intermediate (PII)
September 2019	Microcosms	Add: MPn and TMA	CN, < 3 and CC	Cold room	~ 60	High (PI)

Prior to incubation, initial seawater sampling was taken for each treatment group, wherein triplicate measurements were taken of DO (125 mL), COD (60 mL), chl *a* (100 mL) and nutrients (15 mL). Subsequently, each size-fractionated sample was homogenized and swiftly transferred into 20 mL vials (108 in total, 27 per treatment). These vials were immediately sealed using rubber and aluminum caps to prevent any potential atmospheric gas contamination. The incubation of these vials took place within an FOC 225E incubator, maintained at a temperature of 13 °C and in a 12 h photoperiod (24 h). The illumination was calibrated to fall in a range of 11–11.5 $\mu mol\,m^{-2}\,s^{-1}$ using blue and neutral-density blank filters. At intervals of 4 h, three vials from each treatment (Table 1) were withdrawn and immediately poisoned with 50 µL of $HgCl_2$, and then the vials were gently agitated to ensure homogenization. Gas chromatography was employed to analyze the CH_4 content of the vials. In another set of experiments (Table 1), the picoplankton fraction was singled out to ascertain its capacity for metabolizing methylated substrates and subsequently regenerating CH_4. This involved adding MPn and TMA to the samples. The final concentration of both substrates in these treatments was maintained at 1 µM, assuming that natural concentrations in the seawater were at trace levels. Thus, these could be considered potential experiments (highly enriched). The experimental conditions remained consistent with those employed in the earlier experiment.

2.4 Long-term experiments of CH_4 cycling from size-fractionated planktonic community enriched with organic substrates

Nine microcosms were developed using a system of gas-tight polycarbonate bottles (13 L). Each microcosm contained 10 L of seawater for treatment and 3 L of headspace. They were equipped with a closed gas circuit and connected to a gas spectrometer analyzer capable of simultaneously and continuously measuring various gases, including CO_2, CH_4 and N_2O, and humidity percentage (Fig. 2). Each bottle featured a rubber cap equipped with four holes (as depicted in Fig. 2), housing a 5 mm glass capillary within each hole. These capillaries were connected to gas-tight Teflon hoses. Specifically, the first capillary extended to the middle of the headspace (1) and was linked to an accessory (16-Port Distribution Manifold A0311) of the Picarro G-2308 spectrometer for a cavity ring-down spectroscopy system (CRDS), designed for the measurement of gases in equilibrium with the aqueous phase. The second capillary was suspended within the headspace (2) and connected to a Tedlar bag (3 L) filled with N_2. This arrangement aimed to prevent imbalance when drawing water samples from the microcosm. The third capillary, also suspended in the headspace (3), was equipped with a three-way cannula and was connected to the air outlet of the Picarro G-2308 spectrometer to facilitate the recirculation of air within the headspace. This system optimization aimed to mitigate excessive headspace during spectrometer air sampling, preventing a gas–seawater phase imbalance. This hose (3) was adjustable and replaced upon measuring gas concentrations in each microcosm. The fourth glass capillary was submerged in the seawater, 3 cm from the bottom (4). It was attached to a three-way cannula, streamlining the sample extraction process.

In both April and September of 2019, a series of long-term microcosm experiments were conducted. These months were strategically chosen: the first coinciding with the transition of phytoplankton composition to nano-picoplankton (basal productivity period) and the second with diatom blooms (larger phytoplankton dominance) (high-productivity period), as highlighted in studies by Anabalón et al. (2007), Cuevas et al. (2004), and Morales and Anabalón (2012). The experiment encompassed three distinct treatments: (1) control without any methylated substrate addition in natural communities (NCs), picoplankton community ($< 3\,\mu m$) and picoplanktonic concentrated community (CC); (2) all treatments enriched with MPn; (3) and all treatments enriched with TMA (see Table 1).

The concentrated fraction of picoplankton (CC) was procured through tangential flow filtration via a 0.2 µm filter, following a procedure developed by Giovannoni et al. (1990) for harvesting greater quantities of microbial biomass and using pre-filtering steps as discussed earlier to concentrate only picoplankton ($< 3\,\mu m$). To discern whether the tangential flow

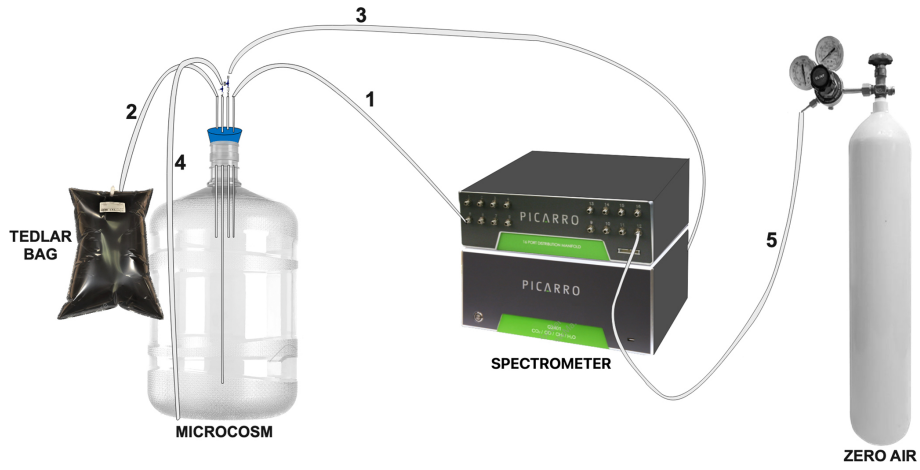

Figure 2. Assembly of the microcosm for long-term experiments (10 L). Capillary 1 is connected directly to the spectrometer. Capillary 2 is connected to a TEDLAR bag filled with N_2 (3 L). Capillary 3 is removable and connected to the outlet of the spectrometer. Capillary 4 is connected to a loose hose for water sampling, and hose 5 is connected to zero air.

filtering was effective, the abundance of cyanobacteria, picoeukaryotes and heterotrophic bacteria was measured with flow cytometry. The incubations were carried out within a controlled cold room environment, maintaining a temperature range of 12 to 13 °C, with the same illumination used in short periods over 60 h. In the initial stages, each bottle was sealed and allowed to acclimate for 6 h in darkness. Following this stage, 1 mL of MPn (10 mM stock solution) and TMA (10 mM stock solution) were introduced to each bottle, yielding a final concentration of 1 µM, matching the conditions established in prior experiments.

To prevent CH_4 residue contamination, a purge with zero air (synthetic air without CH_4 tracers) was performed (as shown in Fig. 2, line 5), ensuring accurate CH_4 concentration measurement within each microcosm and establishing a baseline. Every 4 h a cycle of CH_4 measurements was conducted continuously over 3 min, followed by a 6 min hose cleaning (used for recirculation) with zero air before connecting it to capillary 3 for subsequent measurement. It is important to note that the equipment absorbed 240 mL of air per minute of reading. Therefore, air recirculation within the microcosm, as previously mentioned, was essential. Preceding the actual experiment, the concentrations of gases measured by the spectrometer were closely monitored for 30 min, confirming that the recirculation process did not impact the measured gas concentrations.

2.5 Chemical and biological analysis

2.5.1 Dissolved methane

Once the CH_4 samples were taken, they were stored upside down at room temperature and protected from light and then analyzed through gas chromatography (GC). CH_4 (discrete samples) was determined using the phase equilibrium method (McAuliffe, 1963). In this procedure, each vial was carefully treated, with the addition of 5 mL of inert gas (helium), creating a headspace to facilitate equilibrium between the aqueous and gas phases. Subsequently, the gas phase was measured into a gas chromatography Shimadzu 17 equipped with a flame ionization detector (FID). A Restek Rt-QS-Bond column (30 m length, 0.53 mm inner diameter, 20 µm film thickness) was employed, maintained at a temperature of 30 °C with a flow of 2.6 mL min^{-1} using He as an ultrapure gas carrier.

Five-point calibration curves (linear response of the detector) were made for each monthly sample set (treatment) using a gas with a composition and concentration equivalent to that of the current atmosphere from NOAA (1863.4 ± 0.3 ppbv for CH_4) (Bullister et al., 2016) as the primary standard, as well as three standard gas mixtures (Air Liquide, USA) and zero air. In each CH_4 sample set (every treatment), standards were added at the beginning, middle and end of the measurements to corroborate the correct functioning of the detector. CH_4 measurements (triplicate) with a variation coefficient greater than 10 % were not considered.

2.5.2 Dissolved oxygen

To assess DO content, 125 mL glass flasks were used for sample collection in triplicate. These samples were immediately fixed and analyzed within 6 h of collection through the Winkler method (Carpenter, 1965). The analysis was conducted using a Dosimat 665 instrument featuring an automatic photometric endpoint detector. The detection limit for this method stood at 2 µmol L^{-1}.

2.5.3 Nutrient

Nutrient samples were collected in triplicate using a 60 mL syringe and filtered through a 0.45 µm cellulose acetate filter. The filtered content was held in 15 mL Falcon polyethylene bottles and stored at −20 °C. Analysis of these nutrient samples followed standard colorimetric techniques (Grasshoff et al., 1983) and was conducted using a SealAA3 segmented flow auto-analyzer. This analyzer featured four distinct channels, each equipped with specific modules tailored for individual nutrients.

2.5.4 Chlorophyll *a*

To quantify chl-*a* content, triplicate samples of 100 mL seawater were filtered using a GF/F filter and immediately stored at −20 °C. Analysis was performed according to the method outlined by Holm-Hansen et al. (1965). A Turner Designs 10AU fluorometer was employed for measurement, and a standard pigment served as a reference (Sigma-Aldrich C6144-1MG).

2.5.5 Dissolved organic carbon

For DOC assessment, samples were collected in triplicate using polyethylene bottles. Each 60 mL seawater sample was filtered through a GF/F filter that had been pre-treated by heating at 450 °C for 4 h. After filtration, the samples were acidified to achieve a pH range of 2–3 and stored at −20 °C. Analysis of these samples involved the infrared combustion method using a Shimadzu organic carbon analyzer (TOC-LCPH).

2.5.6 Cytometry

For picoplankton abundance, 3 mL of water was fixed with a glutaraldehyde solution (1 %) and promptly frozen (−80 °C) in liquid nitrogen for storage. Samples were analyzed with flow cytometry using an Influx Cytopeia equipped with five lasers (355, 457, 488, 532, 638 nm). Sort gates were optimized based on the autofluorescence of each group. *Synechococcus sp.* were identified based on their orange fluorescence (530/40 nm) using 488 nm blue and 532 nm green lasers, picoeukaryotes were identified by their red fluorescence (692/40 nm) using 488 nm blue laser, and bacterioplankton were detected using a combination of side scatter light (SSC) (related to cell size) and green fluorescence (530/40 nm).

2.6 Data analysis

2.6.1 Dissolved methane

Dissolved CH_4 concentration was calculated using the solubility coefficient from Wiesenburg and Guinasso (1979). The water column was divided into two layers according to density gradients: (1) well-mixed surface layer (0–20 m) and (2) subsurface layer (20–90 m) from the base of the mixed layer to the bottom, around ∼ 90 m (Farías et al., 2015); this was to interpret the vertical and temporal variability in CH_4.

CH_4 dissolved in the microcosms was measured using continuous sampling connected to the CRDS. Dry mole fractions of CH_4 were converted to concentrations of dissolved CH_4 with the Wiesenburg and Guinasso (1979) solubility coefficient by using in situ temperature and salinity. Each time in the microcosm experiment represents the average of the plateau of each measurement (around 150 and 200 measurements, approximately).

2.6.2 Methane saturation

CH_4 saturation was calculate following Eq. (1):

$$\mathrm{Sat}(\%) = \frac{[\mathrm{CH_4}]_{\text{in situ}}}{[\mathrm{CH_4}]_{\mathrm{eq}}}, \tag{1}$$

where $[CH_4]_{eq}$ was calculated using the solubility coefficient from Wiesenburg and Guinasso (1979).

2.6.3 Methane anomalies and methane hot moments

Monthly anomalies of CH_4 were estimated only in the surface layer, using the following Eq. (2):

$$\mathrm{Anomaly} = \frac{x\mathrm{CH_4} - \bar{x}\mathrm{CH_4}}{\sigma\mathrm{CH_4}}, \tag{2}$$

where $x\mathrm{CH_4}$ is the discrete value at a certain depth (surface) and time (month), $\bar{x}\mathrm{CH_4}$ is the median value for the whole (2018–2021) period at surface, and $\sigma\mathrm{CH_4}$ is the standard deviation of this dataset. CH_4 hot moments were defined as a ΔCH_4 3 times higher than the average monthly value of the anomaly ($\bar{x}\Delta\mathrm{CH_4}$) at each depth within the surface layer as Eq. (3):

$$\frac{\Delta\mathrm{CH_4}}{\bar{x}_{\Delta\mathrm{CH_4}}} > 3, \tag{3}$$

where ΔCH_4 is the disequilibrium of this gas at each depth and was estimated as Eq. (4):

$$\Delta\mathrm{CH_4} = [\mathrm{CH_4}]_{\text{in situ}} - [\mathrm{CH_4}]_{\mathrm{eq}}. \tag{4}$$

2.6.4 Inventories

Inventories of CH_4, chl *a*, and nutrients at the surface (SL) and illuminated layer and subsurface and dark layer (SSL) were calculate through the trapezoidal integration of concentrations of each variable at every layer: minimum three depths in each layer. The averages were taken for DOC because there were only two measurements in each layer.

2.6.5 Methane recycling rates

The net CH_4 recycling rate (net CH_4 accumulation minus CH_4 consumption) in different fractions of the phytoplankton community was calculated through a linear regression of CH_4 concentrations (Farías et al., 2009) during the incubation time (24 h), separating the light cycles (12 h of light and 12 h of darkness).

2.6.6 Methane fluxes

The daily CH_4 flux ($F = \mu mol\, m^{-2}\, d^{-1}$) across the air–sea interface was determined using the equation from Broecker and Peng (1974), modified by Wanninkhof (1992) as follows:

$$F = K_w \cdot (C_w - C^*), \quad (5)$$

where K_w ($cm\, h^{-1}$) is the transfer velocity from the surface water to the atmosphere, as a function of wind speed, temperature and salinity from the mixed layer depth (MLD), where wind speed was obtained from a meteorological station located at Carriel Sur (http://www.meteochile.gob.cl/, last access: May 2022) and MLD was calculated using the potential-density-based criterion of Kara et al. (2003). C_w ($nmol\, L^{-1}$) is the mean CH_4 concentration in the mixed layer, and C^* is the gas concentration in the mixed layer expected to be in equilibrium with the atmosphere according to Wiesenburg and Guinasso (1979). Historical atmospheric values were obtained from registers of gas hemispheric and global monthly means from the NOAA/ESRL program at NOAA (http://www.esrl.noaa.gov, last access: May 2022). More details about the calculation of CH_4 fluxes are found in Farías et al. (2021).

2.6.7 Brunt–Väisälä frequency (BVF)

The Brunt–Väisälä frequency was derived from the observed pressures, temperatures and salinities for each depth set using the TEOS-10 equation of state. This was done in Ocean Data View (ODV v5.6.4) software. Negative values indicate unstable conditions (Schlitzer, 2023).

2.7 Statical analysis

To determine significant differences between the upwelling and non-upwelling periods in both surface and subsurface layers, the non-parametric Mann–Whitney U test was used. To analyze the degree of relationship between oceanographic variables and the variability in CH_4 in the surface layer, Spearman correlations were used. Also, to identify patterns in surface and subsurface variation, a principal component analysis (PCA) was performed. In addition, the Kruskal–Wallis non-parametric statistical test was used to define significant differences between the concentrations given by the different treatments. A statistically significant value was considered $p < 0.05$.

3 Result and discussion

3.1 Oceanographic characteristics related to wind-driven coastal upwelling in central Chile

Figure 3 shows the seasonal variability in DO, stratification, chl *a*, DOC, nutrients and their ratios. Coastal areas off central Chile have a well-documented seasonality of upwelling favorable winds (Strub et al., 1998). Previous studies, based on wind forcing, have identified two distinct seasons: spring–summer (September to April) upwelling and autumn–winter (May to August) non-upwelling (Sobarzo et al., 2007). This seasonality significantly influences temperature, salinity, DO, nutrients and surface chl-*a* concentrations in response to wind-driven stress (Strub et al., 1998; Aguirre et al., 2012). Notably, although most oceanographic variables have clear seasonal patterns, a comparatively weak seasonality is observed in dissolved CH_4 (Fig. 3a).

In the subsurface layer, CH_4 concentrations range from 0.43 to 78.72 nM (mean ± SD = 23.44 ± 15.38 nM; Fig. 3a). These elevated levels could be associated with the seasonal dynamics of organic matter mineralization under hypoxic and suboxic conditions during the upwelling period (spring–summer) (Brown et al., 2014; Capelle and Tortell, 2016; Kock et al., 2008; Farías et al., 2021); however, there are no significant differences in CH_4 accumulations ($p = 0.40$) in subsurface waters during the upwelling (mean ± SD = 22.52 ± 14.34 nM) and non-upwelling (mean ± SD = 24.60 ± 16.65 nM) periods (Fig. 3a). Previously, long-term CH_4 climatology has observed similar values in surface and subsurface layers (Farías et al., 2021).

In the surface layer, there is a highly heterogeneous distribution of CH_4 concentrations, ranging from 0.14 to 41.72 nM (mean ± SD = 11.70 ± 7.79 nM). There are brief events of high CH_4 accumulations within the water column, known as "hot moments" (McClain et al., 2003; referring to disproportionate accumulations over time). CH_4 concentrations during hot moments are between 10.17 nM (390 % saturation) and 41.72 nM (1650 % saturation) and persist during upwelling and non-upwelling periods, as observed in Figs. S1 and S2 in the Supplement. Persistently high CH_4 concentrations in mixing layer depth results in substantial CH_4 effluxes, varying between 3.35 and 23.42 $\mu mol\, m^{-2}\, d^{-1}$ (mean ± SD = 10.10 ± 5.77 $\mu mol\, m^{-2}\, d^{-1}$). When effluxes are estimated and compared for upwelling and non-upwelling periods, there are not significant differences. The lack of seasonal differences in mean surface CH_4 concentrations ($p = 0.63$) and effluxes ($p = 0.23$) could indicate additional input sources, such as river discharges or local surface production. Potentially, the Itata River may contribute to CH_4, DOC and chromophoric dissolved organic matter (DOM; CDOM) discharge (Bello, 2016; Vargas et al., 2016; Rain-Franco et al., 2019), stimulating CH_4 production through aero-

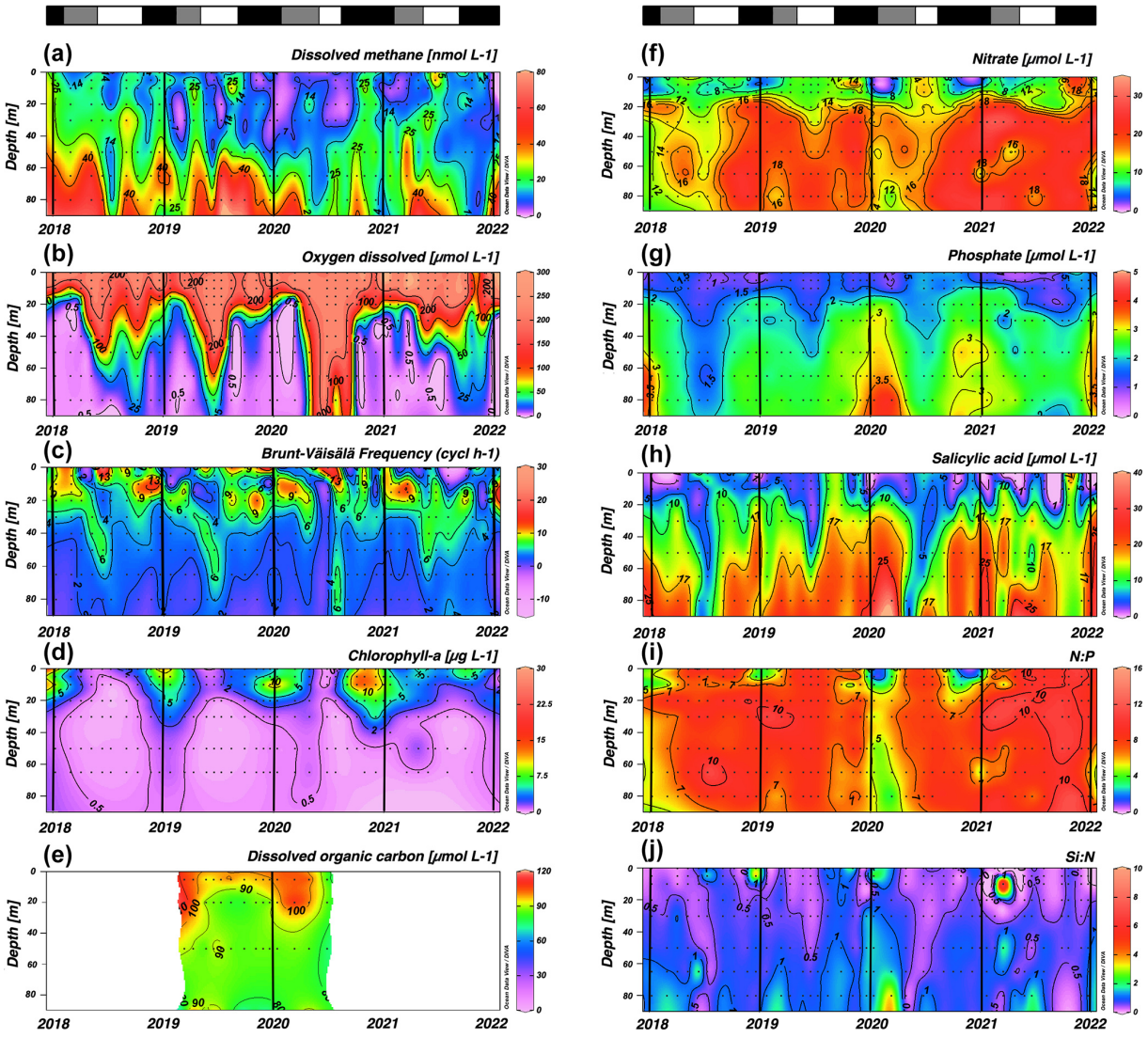

Figure 3. Time series of vertical distributions of **(a)** methane (nmol L^{-1}), **(b)** dissolved oxygen (µmol L^{-1}), **(c)** Brunt–Väisälä frequency (cycles h^{-1}), **(d)** chlorophyll *a* (µg L^{-1}), **(e)** dissolved organic carbon (no purgeable organic carbon – µM), **(f)** nitrate (µmol L^{-1}), **(g)** phosphate (µmol L^{-1}), **(h)** salicylic acid (µmol L^{-1}), N : P ratio and **(j)** Si : N ratio. Sampling was made at ST18 from January 2018 to December 2021. Black lines indicate the start of each year (January). The top bars show different periods' primary production: in black is a high-productivity period (Phase I), in gray is an intermediate-productivity period (Phase II), and in white is a low-productivity period (Phase III).

bic methanogenesis and photooxidation processes (Li et al., 2020; Zhang and Xie, 2015).

CH_4 profiles from samples are shown in Fig. S2. Specific dates present peaks in surface CH_4 over different concentrations, occasionally presenting levels exceeding those in the subsurface layer; so, it is understood that these hot moments in the surface layer are not associated with the vertical advection of CH_4-rich bottom waters.

Thus, it is considered whether hot moments result from physical processes, such as vertical and/or advection associated with upwelling and river discharge, respectively, or biological microbial processes. For the latter, hot moments might be due to in situ aerobic methanogenesis, a process related to the growth and metabolic activities of microalgae (Günthel et al., 2020; Hartmann et al., 2020; Del Valle and Karl, 2014; Bizic, 2021; Cerbin et al., 2022) and bacteria (Repeta et al., 2016; Metcalf et al., 2012; Sun et al., 2019). This type of production is suggested to be a significant reason for CH_4 fluxes in various aquatic systems, including stratified lakes (Grossart et al., 2011; Günthel et al., 2019; Wang et al., 2018) and open oceans (Damm et al., 2010; Karl et al., 2008; Repeta et al., 2016; Sosa et al., 2020; Ye et al., 2020).

Relatively high Brunt–Väisälä frequency (BVF) values (> 10 cycles h^{-1}) are observed between depths of 0 and 20 m,

particularly from September to December (Fig. 3c), whereas subsurface BVF values seem to be associated with annual patterns of thermal stratification, where upwelling from the nearly homogenous ESSW between October and April leads to high-density homogeneity and lower BVF values. During autumn and winter, elevated BVF values are observed in surface waters, probably due to discharge from the Itata River; remarkably there are notably stable values in the subsurface layer (Fig. 3c).

The upper 20 m of the water column has chl-*a* concentrations above $10\,\mu g\,L^{-1}$ (with a marked subsurface peak over different depths) (mean $\pm$ SD 6.60 ± 5.98) in September to January (spring–summer), while lower and more homogeneous values (ranging from 0.5 to $1\,\mu g\,L^{-1}$) are detected during late summer (February to April, mean $\pm$ SD 3.23 ± 2.87) and autumn and winter (May to August, mean $\pm$ SD 1.36 ± 1.91) (Fig. 3d). The study area presents typical DOC concentrations, as expected for highly productive coastal zones (Igarza et al., 2019; Vargas et al., 2013), ranging from 58.79 to 128.63 µM (mean $\pm$ SD $= 90.37 \pm 17.05$) with peak DOC concentrations during late summer and early autumn (Fig. 3e). The surface layer shows reduced but not depleted nutrient concentrations, whereas the subsurface layer presents consistently higher nutrient concentrations (Fig. 3f–h). Within the upper 10 m depth, minimum mean NO_3^- and PO_4^{3-} concentrations occur from September to January and intermediate and higher values between February and August (Fig. 3f and g). These trends are consistent with plankton temporal dynamics (see below). In contrast, $Si(OH)_4$ exhibits higher but heterogeneous concentrations during late autumn and winter and lower values during spring and summer (Fig. 3h). This pattern reflects the high levels of $Si(OH)_4$ associated with river discharges in winter and the development of diatom blooms in spring and summer. CH_4 hot moments occur consistently throughout the year with different stratification scenarios in the water column (Fig. 3a and c) and with different chl-*a* levels (Fig. 3d), revealing a complex interaction between substrates (nutrients and DOC), microorganisms involved and environmental factors (e.g., light, nutrients, water column stability).

Three distinct periods or phases of annual productivity are considered within the study area, based on existing data of primary production, phytoplankton biomass and phytoplankton succession (i.e., changes in composition), related to other biophysical variables (Testa et al., 2018). These periods are September to January (Phase I), with high productivity and chl-*a* biomass, dominated by microplankton including large diatoms, tintinnids and dinoflagellates; from February to April (Phase II) with intermediate productivity, characterized by a shift in plankton composition biomass from larger to smaller organisms, such as flagellates; and from May to August (Phase III), with basal level productivity and relatively low chl-*a* biomass, which corresponds to a non-upwelling period, with a prevalence of pico- and nanoplankton (e.g., *Synechococcus*) including small flagellates and ciliates.

Table 2 presents inventories on CH_4, chl *a*, DOC, NO_3^-, PO_4^{3-}, $Si(OH)_4$ and inorganic nutrient ratios (N : P and Si : N) observed in these periods. The data on chl *a* indicate a marked variation, decreasing from spring to winter (Table 2).

Notably, surface data on DOC show a marginal reduction from Phase I to Phase III (Table 2). It is possible that this fluctuation in DOC accumulation and/or depletion is due to the microbial regeneration exceeding the heterotrophic bacterial consumption (Hansell and Orellana, 2021), or it is attributed to allochthonous sources from rivers (Bauer and Druffel, 1998). Nutrient distribution and concentrations in the surface layer show significant variability among phases (Fig. 3f–h) due to the varied influence by nutrient-rich upwelling events (predominantly observed in spring–summer), biological assimilation and river discharge. These variations significantly affect the N : P and Si : N ratios (Fig. 3i and j), potentially influencing phytoplankton composition. During winter (Phase III), the N : P ratio approaches the expected Redfield stoichiometry, attributed to reduced denitrification in bottom waters (Fernandez et al., 2015) and limited vertical advection towards the surface, contrasting with Phase I. Simultaneously, the Si : N ratio increases due to freshwater discharge from the Itata River (Phase III), encouraging an increase in large diatoms and subsequent $Si(OH)_4$ consumption (Phase I). Considering that hot moments occur throughout different phases and stages of primary production, as well as phytoplankton composition succession (Collado-Fabbri et al., 2011; Aldunate et al., 2018; Anabalón et al., 2007), various levels of chl *a* (see Table 2), and under different nutrient ratios and DOC concentrations (Table 2), it suggests that the conditions and processes favoring the occurrence of hot moments are variables and not entirely clear.

The correlation analysis in the water column showed no significant correlations between CH_4 and the other physicochemical variables (Fig. S3a); however nutrients such as PO_4^{3-} were significantly correlated with T (negative correlation), S (positive correlation), DO (negative correlation) and Si : N ratio (positive correlation) (Fig. S3a), which may be associated with the nutrient-rich, oxygen-poor ESSW. When the surface layer was analyzed in the three productivity periods (Fig. S3b–d), again, no correlation was observed between CH_4 and the other biogeochemical variables; however, in Phases I and II, significant correlations are observed between the nutrients and T, S and DO (negative correlations) (Fig. S3b and c), which may be associated with the upwelling during spring–summer. In Phase III (Fig. S3d), only $Si(OH)_4$ showed significant correlations with T (negative correlation), NO_3^- (positive correlation), PO_4^{3-} (positive correlation) and the Si : N ratio (positive correlation); this may be due to Si input during the rainfall period presented in the autumn–winter period. Moreover, the slight correlation (but no significant) between CH_4 and chl *a* in Phase III suggests that possibly organic matter degradation/con-

Table 2. Average inventories of biogeochemical variables: methane ($\mu mol\,m^{-2}$), chlorophyll *a* ($mg\,m^{-2}$), DOC ($\mu mol\,m^{-2}$), nitrate ($\mu mol\,m^{-2}$), phosphate ($\mu mol\,m^{-2}$), silicate ($\mu mol\,m^{-2}$), and N : P and Si : N ratios, estimated for each productivity period (mean ± SD) from 2018 to 2021. These inventories are estimated for surface layer (SL) and subsurface layer (SSL). Number of hot moments in each period are counted. Phase I: September to January. Phase II: February to April. Phase III: May to August.

Variable	Layer	Productivity periods		
		High Phase I (spring–summer)	Intermediate Phase II (summer–autumn)	Basal Phase III (autumn–winter)
CH_4	SL	265.59 ± 58.36	162.35 ± 21.44	240.54 ± 78.97
	SSL	1315.07 ± 173.69	1012.86 ± 163.23	1275.17 ± 286.38
chl *a*	SL	154.4 ± 102.31	51.32 ± 31.02	26.19 ± 21.17
DOC	SL	114.44 ± 53.94	112.88 ± 8.36	92.41 ± 11.27
	SSL	100.35 ± 46.51	96.97 ± 23.78	86.12 ± 8.95
NO_3^-	SL	260.61 ± 96.25	208.67 ± 49.51	224.65 ± 13.44
	SSL	1274.41 ± 344.24	1033.51 ± 38.5	987.6 ± 113.58
PO_4^{3-}	SL	38.08 ± 10.35	30.29 ± 3.51	28.16 ± 2.99
	SSL	170.22 ± 34.07	137.05 ± 21.57	119.38 ± 11.73
$Si(OH)_4$	SL	131.75 ± 47.07	91.65 ± 38.68	111.24 ± 37.9
	SSL	1065.32 ± 206.98	811.2 ± 225.51	678.07 ± 168.68
N : P	SL	7.69 ± 2.57	7.59 ± 2.44	8.48 ± 0.55
	SSL	9.28 ± 2.52	8.24 ± 0.92	8.46 ± 0.84
Si : N	SL	0.67 ± 0.1	0.69 ± 0.73	0.49 ± 0.15
	SSL	1.04 ± 0.08	1.01 ± 0.26	0.74 ± 0.11
Hot moments	SL	19	9	15

sumption could impact CH_4 production and that low-scale processes (order of hours or days) could mask this correlation, since there is a wide range in the composition of the phytoplankton species involved in CH_4 cycling (Klintzsch et al., 2019, 2023; Günthel et al., 2020).

We further explore the multivariate relationship between CH_4 variability and other variables by separating the data into the surface and subsurface layers by performing a PCA (Fig. S4). Although the CH_4 vector contributes minimally to the total variance in the dataset, distinct behavior is observed in both layers (Fig. S4a and b). In the surface layer, principal component 1 (PC1) shows almost no variability in CH_4 and accounts for 25 % of the total variance. PC2 contains 22.1 % of the total variance and reveals a direct relationship between CH_4 and the variables chl *a*, primary production, Si : N ratio, $Si(OH)_4$, PO_4^{3-} and NO_3^- while being negatively correlated with temperature, DO, NO_2^- and N : P ratio. When separating the dataset into phases, there are differences in variability and the components (Fig. S4c and d). Surface variability is highest in Phase I and lowest in Phase III. Phases I and II vary on both axes, while Phase III is mainly contained on PC2 (Fig. S4c). For the subsurface, the variability is similar in all phases, but the components on which the variability occurs are more differentiated. Phase III varies almost exclusively in the first dimension (the point cloud aligns along the *x* axis), while Phases I and II vary in both dimensions (the point cloud is oblique to the axes) (Fig. S4d); this may be due to the differentiation between the upwelling (Phases I and II) and non-upwelling (Phase III) periods.

So, the complexity inherent in CH_4 dynamics within the study area poses a challenge to comprehension. Consequently, both short- and long-term CH_4 cycling experiments have been conducted to enhance our understanding. These experiments specifically target size-fractioned planktonic communities combined with organic substrates. The objective is to unravel the intricate interactions and substrates that potentially influence CH_4 production. By focusing on size fractions within planktonic communities, it is possible to assess the contribution of diverse groups to CH_4 production.

3.2 Short-term CH_4 cycling within size-fractioned planktonic communities

Figure 4 shows CH_4 accumulation and depletion in plankton-fractionated experiments over a time frame, with daily incubations (12 h of light and 12 h of darkness). Initial experiments were conducted in December 2018 (Fig. 4a) and January 2019 (Fig. 4b), corresponding to a period of high productivity or Phase I (Table S1 in the Supplement) and coin-

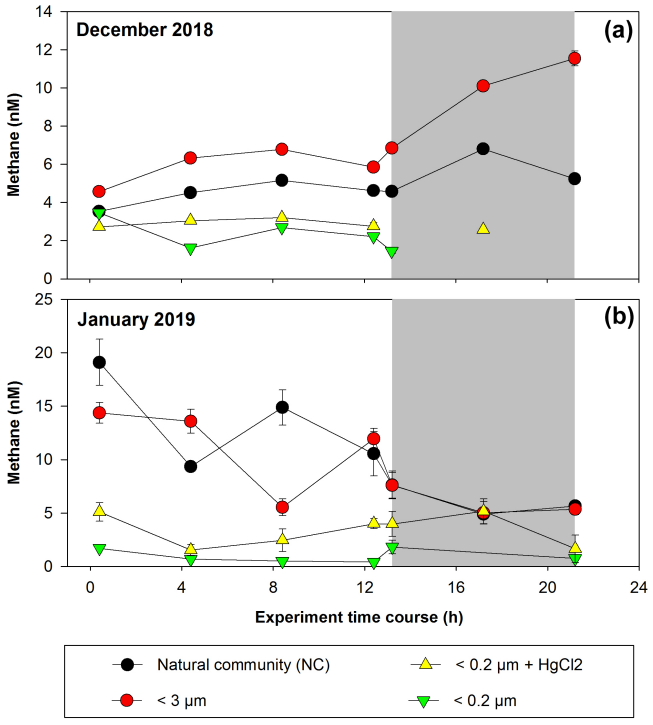

Figure 4. Time courses of dissolved methane concentration (nM) during incubations with fractionated plankton experiments (NC: natural community; < 3 µm: picoplankton and controls (< 0.2 µm)). **(a)** December 2018 and **(b)** January 2019. Photoperiod is represented in white (light) and gray (dark). Error bars represent standard deviation of triplicate samples; when error bars are not visible, they are within the area of the symbol.

ciding with strong vertical advection. The surface water exhibits cooling (∼ 12–13 °C) and elevated CH_4 levels (9.44–17.09 nM), indicative of an active upwelling period (Farías et al., 2021), aligning with other indicators of coastal upwelling (Aguirre et al., 2021).

In the treatments involving fractions < 0.2 µm and < 0.2 µm + $HgCl_2$, which serve as negative controls, CH_4 concentrations remain relatively constant during incubation, with concentrations below 2.32 nM (Fig. 4a) and 5.51 nM (Fig. 4b), indicating biological CH_4 production (Table S2). However, abiotic CH_4 production via photooxidation of CDOM may occur (Li et al., 2020; Zhang and Xie, 2015), but this is not considered in this study. Processes such as DOM photochemical reactions (Mopper et al., 2015), which can contribute to the DOM pool at shallower depths (< 10 m) and be photooxidized to produce CH_4, are disregarded under natural conditions (Li et al., 2020; Zhang and Xie, 2015). In December, CH_4 concentrations in the NC (positive control) and < 3 µm fractions undergo slight increases under light conditions (Fig. 4a; Table S2). However, during darkness, the net CH_4 accumulation is significantly higher in the < 3 µm fraction ($p = 0.03$; Table S2). Picoplankton includes autotrophic and heterotrophic unicellular organisms in the size range of 0.2 to 2 µm. The autotrophic organisms are comprised of cyanobacteria (*Prochlorococcus* and *Synechococcus*) and diverse picoeukaryotes larger than 1 µm (Worden, 2006), while the heterotrophic organisms are primarily prokaryotes, with bacteria overwhelmingly dominating over archaea in the upper layers (Smith et al., 2013). This fraction (< 3 µm) includes several coexisting metabolic groups that depend on different energy sources such as sunlight, DOC or even a combination of the two (mixotrophy). These groups are critical for the functioning of the microbial food web and are predominantly responsible for DOC cycling (Muñoz-Marín et al., 2020; Reintjes et al., 2020) and its derivative compounds (including CH_4).

In January, the experiments show distinct results, with CH_4 levels decreasing over incubation time in both the NC and < 3 µm fractions for both photoperiods (Fig. 4b), although the rate of consumption is lower in darkness (Table S2). These differences suggest that the composition of the microbial community during the high-productivity period, as well as the quantity and quality of DOC and nutrient concentrations and their ratios (Allen et al., 2012; Spilling et al., 2019), controls CH_4 cycling. Indeed, the environmental conditions differ during sampling (Table S1); although both months are oxygenated, both vary in chl-*a* and nutrient levels, including CH_4 (Fig. 3c; Table S1).

Significant differences in CH_4 accumulation rates between the NC and < 150 µm fraction treatments (data not shown) are observed compared with the < 3 µm fraction (Table S2). Peak cycling rates occur in the < 3 µm fraction, indicating that larger microorganisms do not affect the net CH_4 accumulation and consumption (Table S2), highlighting the importance of the microbial loop in CH_4 cycling. Additionally, the observed differences between photoperiods in both fractions may suggest coupling mechanisms between autotrophic phytoplankton and heterotrophic bacterioplankton communities (León-Palmero et al., 2020; Morán et al., 2002; Repeta et al., 2016).

CH_4 consumption by methanotrophs should be considered in CH_4 cycling experiments, as aerobic CH_4 oxidation significantly reduces the net CH_4 accumulation rates (net production vs. consumption) (Mao et al., 2022). While the impact of light on methanotrophs is not widely understood (Broman et al., 2023), the existing literature suggests that methanotrophs may experience inhibition under light conditions (Dumestre et al., 1999; Morana et al., 2020). Consequently, CH_4 accumulation should be higher under these conditions. However, this does not agree with our results (for light and dark conditions), indicating that methylotrophs are more dynamic and complex than expected, making them difficult to understand through the observation of their daily cycles.

3.3 Short-term CH_4 cycling experiment from picoplankton amended with organic substrates

As the picoplankton fraction showed the highest rate of CH_4 accumulation (Fig. 4), this prompts its selection for assessing its potential for methylotrophic methanogenesis through the addition of methylated substrates (MPn and TMA) in a daily cycle. Phosphonate (MPn) and methylamine compounds (mono-, di- and trimethylamines) are dissolved methylated compounds known to stimulate CH_4 production because they have a methyl radical ($-CH_3$), a potential precursor for CH_4 formation in oxygenated environments (Karl et al., 2008; Repeta et al., 2016; Wang et al., 2021; Bižić-Ionescu et al., 2018).

These compounds are ubiquitous in various ecosystems (Lohrer et al., 2020; Sun et al., 2019), yet they have distinct metabolic origins. The MPn originates from microorganisms as Archaea *Nitrosopumilus maritimus* (Metcalf et al., 2012) and *Candidatus pelagibacter spp.* (Born et al., 2017), two of the most abundant marine microorganisms. MPn is found at very low concentrations ($\sim 0.01\,\mu M$, close to its analytical detection limit) likely due to rapid microbial turnover (Karl et al., 2008; Martínez et al., 2013; Urata et al., 2022). The methylamine compounds like the trimethylamine compounds exhibit a wide concentration range in the ocean, from nM levels in the open ocean to µM levels in sediments and near the coast (Sun et al., 2019). Environmental TMA concentrations could be higher, particularly in upwelling regions that bring the TMA from bottom waters to the surface (Gibb et al., 1999; Sun et al., 2019). In this context, the amendments performed for each substrate, 100-fold for MPn and 1000-fold for TMA, convert these experiments into potential rates.

These amendment experiments were conducted in Phase II (March 2019) and Phase III (May 2019), periods of change in phytoplankton succession (composition), biomass and abundance (Testa et al., 2018). In winter, the relative abundance of picoplankton with respect to microplankton (particularly the presence of *Synechococcus* and nitrifying archaea) increases significantly, especially photosynthetic picoeukaryotes (Collado-Fabbri et al., 2011). The time course CH_4 accumulation during incubations is illustrated in Fig. 5. We observe highly variable temporal fluctuations during these periods (March and May). A particularity is the abrupt increase in CH_4 concentration upon transitioning from light to dark cycles in March (Phase II), as well as the significant CH_4 accumulation that persists in darkness (Fig. 5a). In May (Phase III), the time course distribution of CH_4 in each treatment exhibits considerable variability. Notably, the addition of MPn results in greater accumulation in CH_4, particularly in darkness, accompanied by a pronounced increase over incubation time (Fig. 5b; Table S2). In both periods, the $< 3\,\mu m + MPn$ treatment exhibits contrasting patterns under dark conditions (Figs. 5a and 4b), decreasing in Phase II and increasing in Phase III, suggesting the importance of microbial composition. During winter (Phase III), a higher DOC concentration is found (Fig. 3e), which may lead to higher bacterial and archaeal activity that could be metabolizing DOC, including MPn under dark conditions. On the other hand, despite a coefficient of variation $< 10\,\%$, we cannot entirely discount experimental issues in the abrupt rise of the $< 3\,\mu m + MPn$ treatment at around 12 h.

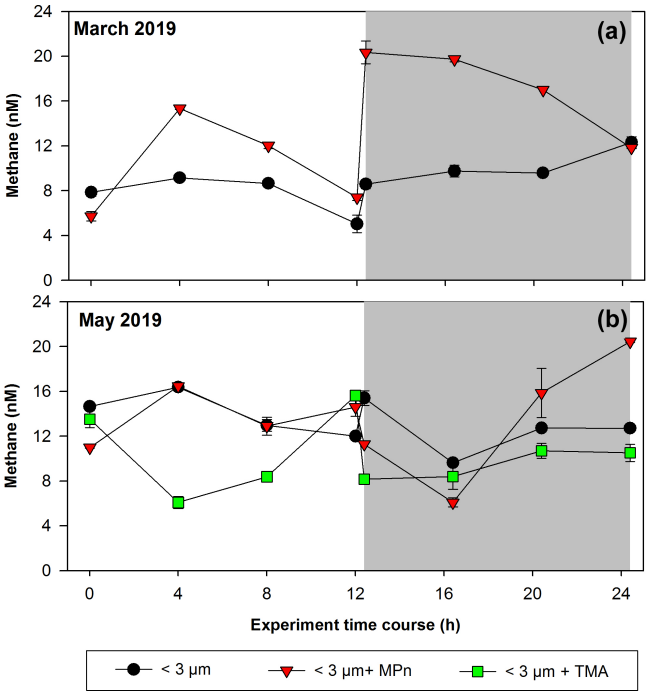

Figure 5. Time courses of dissolved methane concentration (nM) during incubations with the addition of methylated substrates (MPn: methyl phosphonic acid; TMA: trimethylamine) performed with bacterioplankton ($< 3\,\mu m$) and bacterioplankton concentrate (CC). **(a)** March 2019 and **(b)** May 2019. Photoperiod is represented in white (light) and gray (dark). Error bars represent standard deviation of triplicate samples; when error bars are not visible, they are within the area of the symbol.

Conversely, the TMA treatment does not result in any CH_4 accumulation, being lower compared to the control and MPn treatments (Fig. 5b); while TMA can be metabolized by marine bacteria (Lidbury et al., 2015; Bižić-Ionescu et al., 2018), the reduced CH_4 production in this treatment suggests an end product different than CH_4 (Sun et al., 2019). In contrast, heterotrophic picoplankton might metabolize MPn and produce CH_4, showing in situ methanogenesis via the carbon–phosphorus (C–P) lyase pathway (Karl et al., 2008).

3.4 Long-term CH_4 cycling from concentrated picoplankton amended with organic substrates

For a more comprehensive understanding, our study involves long-term microcosm experiments conducted during two distinct phases of productivity. One of these phases oc-

curs during intermediate productivity (Phase II or late summer to autumn), characterized by a notable prevalence of autotrophic small diatoms, picoeukaryotes and cyanobacteria (*Synechococcus*), in contrast to the high-productivity period (Phase I or early springtime) (Fig. S5a and d), when large diatoms are predominant (Fig. S5b and e), while heterotrophic bacterioplankton exhibits an almost constant presence in both periods (Fig. S5c and f). These temporal distributions align with well-documented phytoplankton and bacterioplankton patterns in our study area (Aldunate et al., 2018; Collado-Fabbri et al., 2011; De La Iglesia et al., 2020; Molina et al., 2020).

Briefly, Flavobacteriaceae, SAR11 subclade IA (*Candidatus Pelagibacter spp.*), SAR11 subclade 1b, gammaproteobacterial clades and SAR86 are prevalent during upwelling seasons, while during non-upwelling seasons or Phase III, SAR11 subclade II, marine Actinobacteria and unclassified Alphaproteobacteria dominate (Aldunate et al., 2018). In addition, photosynthetic picoplankton eukaryotes related to Mamiellophyceae (*Bathycoccus*, *Micromonas* and *Ostreococcus*) are predominantly observed with high significance in the surface layer during the transition period (Collado-Fabbri et al., 2011; De La Iglesia et al., 2020), whereas the abundance of heterotrophic bacteria, ranging from 0.23 to 6.50×10^6 cells mL^{-1}, is mainly concentrated in the surface during late summer and autumn, with minima in winter (Molina et al., 2020). However, in our study, the abundance of heterotrophic bacteria shows no significant differences ($p = 0.05$) in both periods (1×10^6 cells mL^{-1}) (Fig. S5c and f). This is due to the low DOC at the beginning of the upwelling period (Fig. 3e).

The CH_4 accumulations during time incubations under different treatments in Phase II are illustrated in Fig. 6. Net CH_4 cycling rates are detailed in Table S4. Variations are observed when these rates are differentiated between light and dark periods, as well as across different periods or phases of productivity (Table S4). The concentrated community (CC) results in substantial enrichments of cyanobacteria (*Synechococcus*), picoeukaryotes and heterotrophic bacteria by factors of 1.9, 1.8 and 4.6, respectively, compared to the NC and factors of 1.8, 1.8 and 6.1, respectively, in relation to the natural < 3 µm fraction (Fig. S5a–c). In both cases, a significant increase in bacteria is observed (Fig. S5c). The microbial abundance proportions in the NC treatment at the beginning of the experiment closely align with field observations (Collado-Fabbri et al., 2011; Anabalón et al., 2007; Morales et al., 2007; Morales and Anabalón, 2012).

Mean chl-*a* levels in the < 3 µm fraction are 21.7 and 4.5 times lower than in the NC and CC, respectively (Table S3). This suggests that this fraction contains phytopicoeukaryotes (e.g., coccolithophorids, cryptophytes) and picocyanobacteria (e.g., *Synechococcus*) in a lower proportion than the CC. Additionally, the CC treatment displays higher background levels of DOC and nutrients probably due to the natural diurnal mortality of picoplankton (Llabrés et al., 2011). It cannot be ruled out that the baseline is due to tangential flow filtration, although it is one of the most used methods to concentrate DOM (Benner et al., 1992), reducing the amount of membrane sorption and fouling (Minor et al., 2014).

In April (Phase II), CH_4 cycling rates consistently exhibit higher values during the dark phase, suggesting a significant involvement of heterotrophic bacterioplankton (Table S4). Additionally, these rates are notably elevated in the CC treatments, particularly in the CC + MPn (Table S4). When comparing the treatments (NC, < 3 µm and CC) without (controls) and with the addition of MPn and TMA (Fig. 6; Table S4), although temporal patterns are similar, significant differences between treatments ($p = 0.002$) are found with slightly higher CH_4 cycling rates in < 3 µm in dark conditions (Fig. 6a; Table S4). With the addition of MPn (Fig. 6b; Table S4), the CC + MPn treatment, characterized by the highest abundance of autotrophic (cyanobacteria) and heterotrophic microorganisms (Fig. S5), exhibits a significant increase in a net CH_4 accumulation in both light and dark conditions (Table S4). In addition, higher chl-*a* concentrations (Table S3) in the NC treatment may have supported greater CH_4 accumulation compared to the < 3 µm fraction (Fig. 6b). Regarding the TMA enrichment (Fig. 6c), both the CC and the < 3 µm fraction treatments respond similarly, increasing CH_4 concentration over time ($p = 3 \times 10^{-6}$; Fig. 6c) although the recycling rates were slightly higher in < 3 µm + TMA, suggesting that microbial abundance does not significantly affect CH_4 production with TMA or that the heterotrophic community in the CC treatment weakly metabolizes TMA (De Angelis and Lee, 1994; Bižić-Ionescu et al., 2018).

Although the metabolization of methylated substrates, such as MPn to CH_4 by various types of bacteria, has been extensively documented (Repeta et al., 2016; Del Valle and Karl, 2014; Metcalf et al., 2012; Zhao et al., 2022; Damm et al., 2010; Karl et al., 2008), this has only been reported mostly under phosphorus-starved conditions. However, this is unlikely in our study area, which experienced high PO_4^{3-} availability, even in excess compared to N (Table 2). Specifically, the expression of phosphonate C–P lyase genes could arise when P-starved (Carini et al., 2014; Taenzer et al., 2020; Sosa et al., 2019). Thus, an alternative explanation for the significant CH_4 accumulation in the CC with MPn treatment could be related to the presence of photosynthetic cyanobacteria (Bižić et al., 2020), which have adaptive strategies to fluctuating P levels (Li and Dittrich, 2019). This is further complemented by the capacity of some bacteria to degrade phosphonates in environments with a substantial background of P (Schowanek and Verstraete, 1990).

Given that *Synechococcus* dominates during the non-upwelling period (autumn–winter season) in the photic layer (Collado-Fabbri et al., 2011), it becomes plausible to consider CH_4 production mediated by this microorganism in this period. Consequently, CH_4 production pathways appear

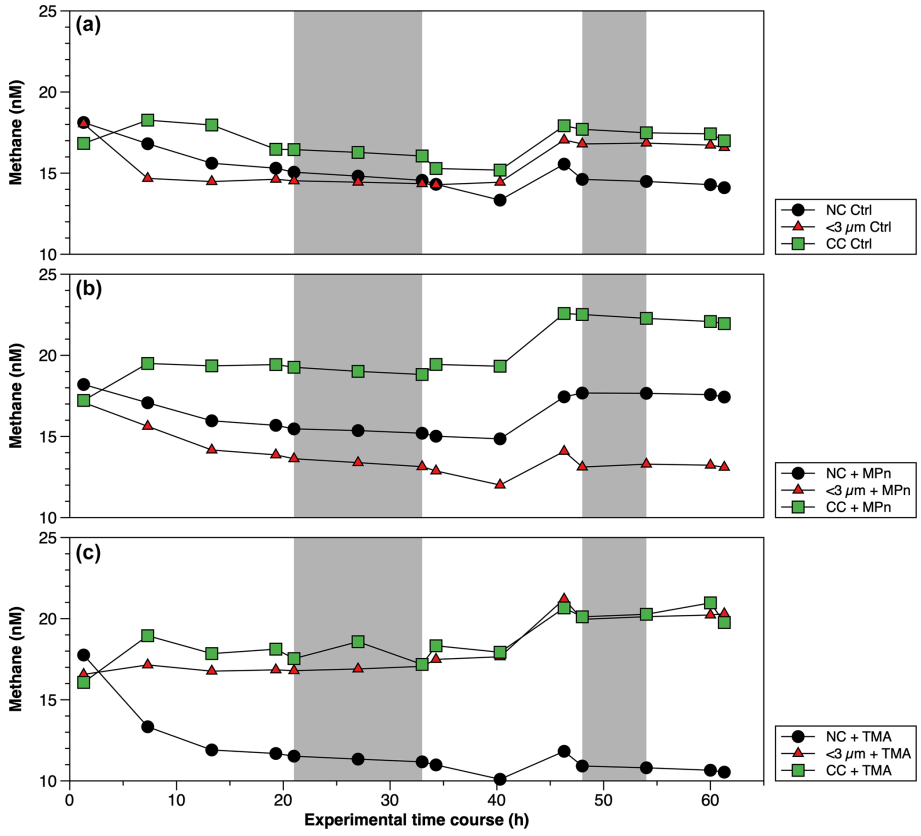

Figure 6. Time courses of dissolved methane (nM) during incubation in long-term microcosm experiments (10 L) with the addition of methylated substrates (MPn: methyl phosphonic acid; TMA: trimethylamine) performed with three planktonic communities (NC: natural community; < 3 µm: bacterioplankton; CC: community concentrate) under oxygenated conditions in April 2019. Photoperiod is represented in white (light) and gray (dark).

multifaceted, involving complex interplays between photochemical and metabolic processes. The mechanism by which cyanobacteria effectively convert fixed CO_2 to CH_4 under light conditions appears intricately linked to the photosynthetic process (Bižić et al., 2020; Klintzsch et al., 2020) as inhibitors of photosynthesis blocked CH_4 production under light conditions (Bižić et al., 2020). They suggest that distinct mechanisms might govern CH_4 production under light and dark conditions, influenced by freshly synthesized photosynthetic products in light and storage compounds during darkness.

In September (Phase I), CH_4 cycling rates exhibit substantial differences compared to those estimated for Phase II. Notably, these rates are lower in most treatments, with a reversal observed in the pattern compared to Phase II; i.e., CH_4 cycling rates during light conditions surpass those during dark conditions (Table S4). Furthermore, the CC treatments consistently demonstrate the highest rates compared to the other treatments (Table S4). Temporal CH_4 accumulation in this phase consistently demonstrates higher CH_4 levels in the CC treatment compared to the NC and < 3 µm fraction (controls) (Fig. 7a). However, a noteworthy contrast appears when considering the impact of substrate additions. Specifically, the addition of TMA in the CC treatment in this phase results in a more pronounced CH_4 production (Fig. 7c) compared to the effect of MPn (Fig. 7b), especially in dark conditions (Table S4). This pattern, the opposite of that found in Phase II, could potentially be explained by the observed decrease in *Synechococcus* abundance (Fig. S5d), which remains unresponsive to MPn, and the concurrent increase in nano- and picoeukaryotes and bacteria at the end of the experiment (Fig. S5e and f), the last of which could be conducive to the action of TMA (Bižić-Ionescu et al., 2018; De Angelis and Lee, 1994; Lidbury et al., 2015). Indeed, a marked reduction in *Synechococcus* abundance is observed (showing a 4.6-fold decrease) compared to Phase II (Fig. S5a and d), whereas nano- and picoeukaryotes experience notable abundance (3.1 to 3.7 times higher than the transition period) (Fig. S5b and e).

In this phase, the distribution proportions within the NC treatment are cyanobacteria, nano- and picoeukaryotes, and bacteria accounting for 1.1, 2.3 and 96.6, respectively. In contrast, within the CC treatment, the initial distribution proportions are higher with respect to the NC: cyanobac-

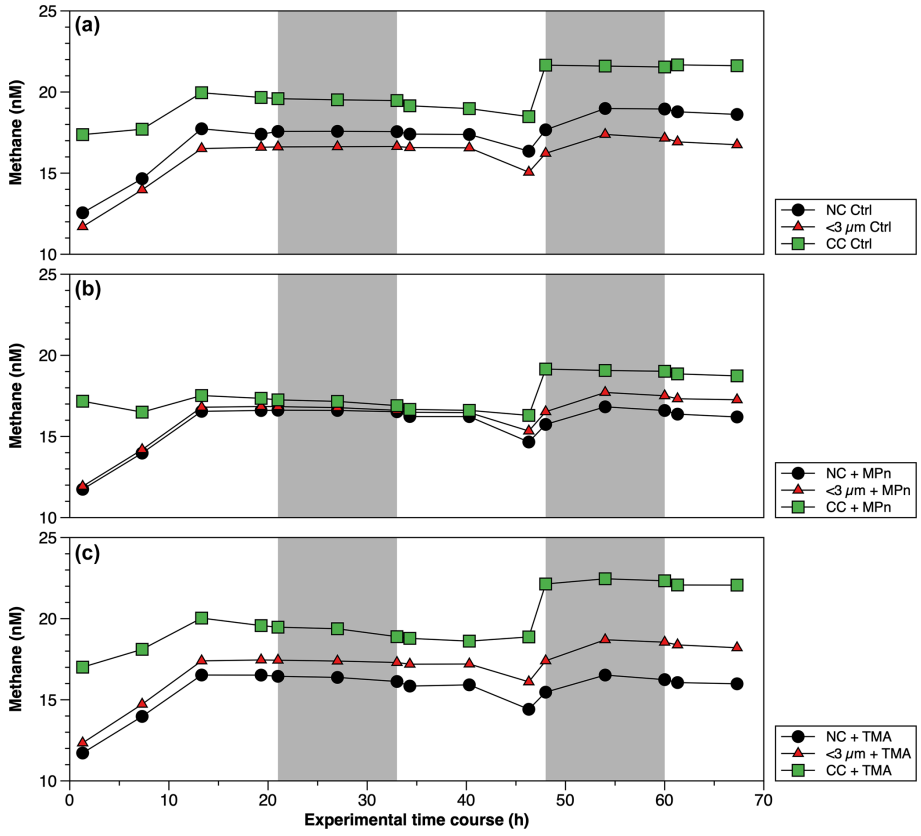

Figure 7. Time courses of dissolved methane (nM) during incubation in long-term microcosm experiments (10 L) with the addition of methylated substrates (MPn: methyl phosphonic acid; TMA: trimethylamine) performed with three planktonic communities (NC: natural community; < 3 µm: bacterioplankton; CC: community concentrate) under oxygenated conditions in September 2019. Photoperiod is represented in white (light) and gray (dark).

teria, picoeukaryotes and bacterioplankton displayed proportions 1.6, 0.6 and 2.9 times greater, respectively. This underscores the increased significance of bacteria and autotrophic picoeukaryotes during this phase, as further corroborated by chl-*a* measurements (Table S3). An intricate interplay between microbial communities and CH_4 cycling within distinct phases of productivity is schematically illustrate in Fig. 8. The prevalence of cyanobacteria, picoeukaryotes and heterotrophic bacteria varied significantly between these phases. So, this indicates that substrate utilization is related to the availability of nutrients as well as the complexity of the substrate and the composition of the heterotrophic bacterial community, potentially driving CH_4 production dynamics.

High CH_4 levels in surface water during the non-upwelling period, comparable to the upwelling period, could result from in situ CH_4 production mediated by photosynthetic *Synechococcus* or demethylation by heterotrophic bacteria (Fig. 8a). On the other hand, although the trimethylamine methyltransferase enzyme has been described as being involved in the demethylation of TMA in methanogen microorganisms (Paul et al., 2000), it cannot be ruled out that in Phase I (spring) heterotrophic bacteria dominance can metabolize TMA through an alternative pathway still unknown (Fig. 8b), nor can it be ruled out that the upwelling brings methanogens with the necessary machinery to metabolize TMA at the ocean surface.

4 Conclusions

Overall, picoplankton produced CH_4 in all experiments conducted in both light and dark conditions, although the net CH_4 production rate was higher in dark conditions. Moreover, laboratory experiments demonstrated that organic compounds such as TMA and MPn are metabolized by heterotrophic bacterioplankton, contributing to the production of oxic CH_4 in the oxygenated surface layer.

Coastal upwelling could bring with it organic amino compounds such as TMA including mono- and di-trimethylamines from sediments, which added to plankton decomposition compounds, and the change in picoplanktonic composition (bacteria and the remarkable increase in pico- and nano-eukaryotes) during the favorable upwelling period could promote CH_4 production via TMA, through a path-

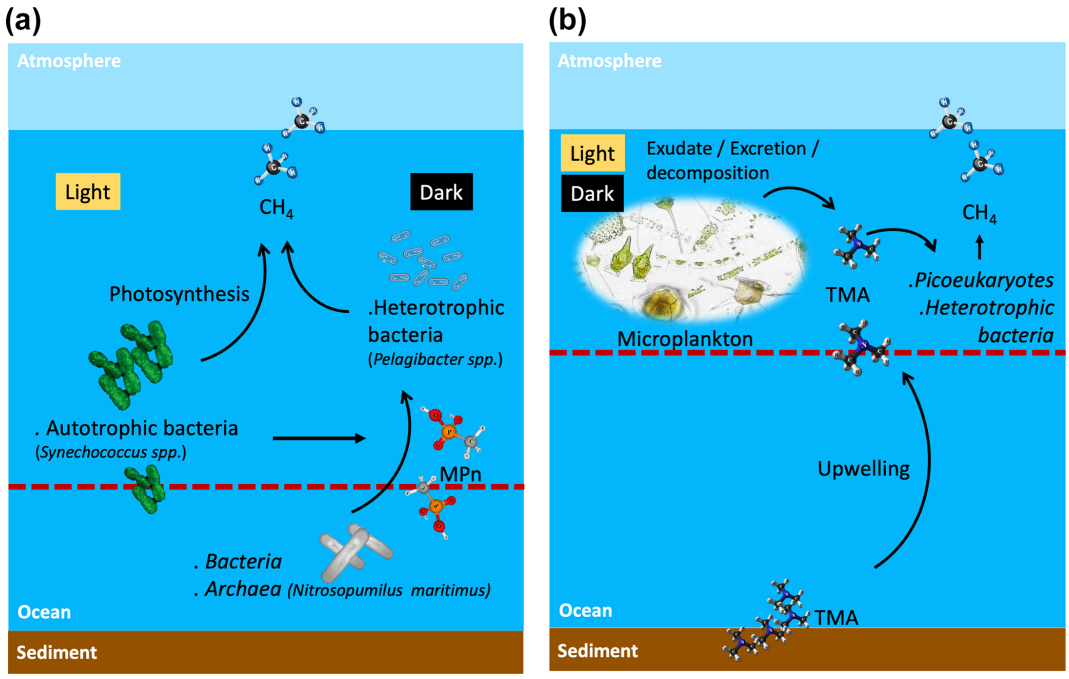

Figure 8. Suggested scheme of methane cycling mechanisms in two contrasting periods of primary production and oceanographic conditions during light and dark phases, where potential planktonic communities and methylated substrates are involved to metabolize methane in surface waters. **(a)** Phases II and III or late upwelling or non-upwelling season and **(b)** Phase I or active upwelling season. Dashed line shows the 100 µmol L^{-1} oxycline, above this line oxic methane is produced. TMA: trimethylamine; MPn: methyl phosphonic acid.

way that is still unknown, but would potentially add to CH_4 supersaturation in the oxygenated surface layer, beyond the contribution of CH_4 by advection.

Synechococcus could be responsible for CH_4 regeneration through photosynthesis. These cyanobacteria are abundant in the non-upwelling period and, together with other picoeukaryotes, maintain intermediate and basal chl-*a* levels during this period that matched with higher DOC levels and inorganic N : P ratios (compared to the upwelling period). This may stimulate heterotrophic bacteria to metabolize MPn and thus contribute to the recycling of oxic CH_4.

It is important to note that amended experiments were conducted in Phase II (March 2019) and Phase III (May 2019), periods marked by changes in the phytoplankton succession (composition), biomass and abundance in winter; the relative abundance of picoplankton with respect to microplankton (particularly the presence of *Synechococcus* and nitrifying archaea) increases significantly, especially photosynthetic picoeukaryotes.

Data availability. All raw data can be provided by the corresponding authors upon request.

Supplement. The supplement related to this article is available online at: https://doi.org/10.5194/bg-21-2029-2024-supplement.

Author contributions. SET and LF designed the experiments, and SET carried them out, performed the measurements, analyzed the data, and drafted the manuscript. LF reviewed and edited the manuscript.

Competing interests. The contact author has declared that neither of the authors has any competing interests.

Disclaimer. Publisher's note: Copernicus Publications remains neutral with regard to jurisdictional claims made in the text, published maps, institutional affiliations, or any other geographical representation in this paper. While Copernicus Publications makes every effort to include appropriate place names, the final responsibility lies with the authors.

Acknowledgements. Thanks to Gerardo Garcia for his experience and teaching in the use of laboratory equipment and his help in setting up the experiments; Karen Sanzana for nutrient analysis; and Oliver Alarcon for oxygen analysis. Both the crew of RV *Kay–Kay II* and the Dichato Marine Station of the University of Concepción provided valuable help during fieldwork, as well as all participating colleagues in the time series station (University of Concepción), who provided the core measurements. We also appreciate the work done during the COVID pandemic by Juan Faúndez.

Financial support. This research was funded by the Fondo Nacional de Desarrollo Científico y Tecnológico (FONDECYT) grant no. 1200861 and also Millennium Science Initiative Program ICM 2019-015 (SECOS) and CR2 FONDAP-CONICYT no. 1522A001.

Review statement. This paper was edited by Hermann Bange and reviewed by two anonymous referees.

References

Aguirre, C., Pizarro, Ó., Strub, P. T., Garreaud, R., and Barth, J. A.: Seasonal dynamics of the near-surface alongshore flow off central Chile, J. Geophys. Res.-Oceans, 117, C01006, https://doi.org/10.1029/2011JC007379, 2012.

Aguirre, C., Garreaud, R., Belmar, L., Farías, L., Ramajo, L., and Barrera, F.: High-frequency variability of the surface ocean properties off central Chile during the upwelling season, Front. Mar. Sci., 8, 1–19, https://doi.org/10.3389/fmars.2021.702051, 2021.

Aldunate, M., De la Iglesia, R., Bertagnolli, A. D., and Ulloa, O.: Oxygen modulates bacterial community composition in the coastal upwelling waters off central Chile, Deep-Sea Res. Pt. II, 156, 68–79, https://doi.org/10.1016/j.dsr2.2018.02.001, 2018.

Allen, L. Z., Allen, E. E., Badger, J. H., McCrow, J. P., Paulsen, I. T., Elbourne, L. D., Thiagarajan, M., Rusch, D. B., Nealson, K. H., Williamson, S. J., Venter, J. C., and Allen, A. E.: Influence of nutrients and currents on the genomic composition of microbes across an upwelling mosaic, ISME J., 6, 1403–1414, https://doi.org/10.1038/ismej.2011.201, 2012.

Anabalón, V., Morales, C. E., Escribano, R., Varas, A. M., and Varas, M. A.: The contribution of nano- and microplanktonic assemblages in the surface layer (0–30 m) under different hydrographic conditions in the upwelling area off Concepción, central Chile, Prog. Oceanogr., 75, 396–414, https://doi.org/10.1016/j.pocean.2007.08.023, 2007.

Bange, H. W., Bartell, U. H., Rapsomanikis, S., and Andreae, M. O.: Methane in the Baltic and North Seas and a reassessment of the marine emissions of methane, Global Biogeochem. Cy., 8, 465–480, 1994.

Bauer, J. and Druffel, E.: Ocean margins as a significant source of organic matter to the deep open ocean, Letter to Nature, 392, 482–485, https://doi.org/10.1038/33122, 1998.

Bello, E.: Variabilidad estacional en la descarga de metano disuelto desde un sistema estuarino a la zona marina adyacente, el caso de ríos de la zona central de chile (río Itata), Universidad de Concepción, 76 pp., http://repositorio.udec.cl/jspui/handle/11594/10347 (last access: 18 April 2024), 2016.

Belviso, S., Kim, S.-K., Rassoulzadegan, F., Krajka, B., Nguyen, B. C., Mihalopoulos, N., and Buat-Menard, P.: Production of dimethylsulfonium propionate (DMSP) and dimethylsulfide (DMS) by a microbial food web, Limnol. Oceanogr., 35, 1810–1821, https://doi.org/10.4319/lo.1990.35.8.1810, 1990.

Benner, R., Dean Pakulski, J., Mccarthy, M., Hedges, J. I., Hatcher, P. G., Benner, R., Pakulski, J. D., McCarthy, M., Hedges, J. I., Hatcher, P. G., H van Beest, B. W., Kramer, G. J., and van Santen, R. A.: Bulk chemical characteristics of dissolved organic matter in the ocean, Science, 255, 1561–1564, https://doi.org/10.1126/science.255.5051.1561, 1992.

Berg, A., Lindblad, P., and Svensson, B. H.: Cyanobacteria as a source of hydrogen for methane formation, World J. Microb. Biot., 30, 539–545, https://doi.org/10.1007/s11274-013-1463-5, 2014.

Bianchi, T. S.: The role of terrestrially derived organic carbon in the coastal ocean: A changing paradigm and the priming effect, P. Natl. Acad. Sci. USA, 108, 19473–19481, https://doi.org/10.1073/pnas.1017982108, 2011.

Bizic, M.: Phytoplankton photosynthesis: An unexplored source of biogenic methane emission from oxic environments, J. Plankton Res., 43, 822–830, https://doi.org/10.1093/plankt/fbab069, 2021.

Bižić, M., Klintzsch, T., Ionescu, D., Hindiyeh, M. Y., Günthel, M., Muro-Pastor, A. M., Eckert, W., Urich, T., Keppler, F., and Grossart, H. P.: Aquatic and terrestrial cyanobacteria produce methane, Sci. Adv., 6, 1–10, https://doi.org/10.1126/sciadv.aax5343, 2020.

Bižić-Ionescu, M., Ionescu, D., Günthel, M., Tang, K. W., and Grossart, H. P.: Oxic methane cycling: new evidence for methane formation in oxic lake water, in: Biogenesis of Hydrocarbons, Handbook of Hydrocarbon and Lipid Microbiology, edited by: Stams, A. J. M. and Souza, D. Z., Springer International Publishing AG, part of Springer Nature, 1–22, https://doi.org/10.1007/978-3-319-53114-4_10-1, 2018.

Borges, A. V. and Abril, G.: Carbon Dioxide and Methane Dynamics in Estuaries, in: Treatise on Estuarine and Coastal Science, vol. 5, edited by: Wolanski, E. and McLusky, D., Elsevier Inc. Academic Press, 119–161, https://doi.org/10.1016/B978-0-12-374711-2.00504-0, 2012.

Born, D. A., Ulrich, E. C., Ju, K. S., Peck, S. C., Van Der Donk, W. A., and Drennan, C. L.: Structural basis for methylphosphonate biosynthesis, Science, 358, 1336–1339, https://doi.org/10.1126/science.aao3435, 2017.

Broecker, W. S. and Peng, T. H.: Gas exchange rates between air and sea, Tellus, 26, 21–35, https://doi.org/10.1111/j.2153-3490.1974.tb01640.x, 1974.

Broman, E., Barua, R., Donald, D., Roth, F., Humborg, C., Norkko, A., Jilbert, T., Bonaglia, S., and Nascimento, F. J. A.: No evidence of light inhibition on aerobic methanotrophs in coastal sediments using eDNA and eRNA, Environmental DNA, 5, 766–781, https://doi.org/10.1002/edn3.441, 2023.

Brown, I. J., Torres, R., and Rees, A. P.: The origin of sub-surface source waters define the sea-air flux of methane in the Mauritanian Upwelling, NW Africa, Dynam. Atmos. Oceans, 67, 39–46, https://doi.org/10.1016/j.dynatmoce.2014.06.001, 2014.

Bullister, J. L., Wisegarver, D. P., and Wilson, S. T.: The production of methane and nitrous oxide gas standards for Scientific Committee on Ocean Research (SCOR) Working Group #143, Pacific Marine Environmental Laboratory (NOAA-PMEL) for SCOR WG 143, Seattle, WA, 1–9, https://doi.org/10.25607/OBP-24, 2016.

Capelle, D. W. and Tortell, P. D.: Factors controlling methane and nitrous-oxide variability in the southern British Columbia coastal upwelling system, Mar. Chem., 179, 56–67, https://doi.org/10.1016/j.marchem.2016.01.011, 2016.

Capone, D. G. and Hutchins, D. A.: Microbial biogeochemistry of coastal upwelling regimes in a changing ocean, Nat. Geosci., 6, 711–717, https://doi.org/10.1038/ngeo1916, 2013.

Carini, P., White, A. E., Campbell, E. O., and Giovannoni, S. J.: Methane production by phosphate-starved SAR11

chemoheterotrophic marine bacteria, Nat. Commun., 5, 1–7, https://doi.org/10.1038/ncomms5346, 2014.

Carpenter, J.: Do rats and pigeons readily acquire instrumental responses for food in the presence of free food?, Limnol. Oceanogr., 10, 141–143, https://doi.org/10.3758/BF03209628, 1965.

Carpenter, L. J., Archer, S. D., and Beale, R.: Ocean-atmosphere trace gas exchange, Chem. Soc. Rev., 41, 6473–6506, https://doi.org/10.1039/c2cs35121h, 2012.

Cerbin, S., Pérez, G., Rybak, M., Wejnerowski, Ł., Konowalczyk, A., Helmsing, N., Naus-Wiezer, S., Meima-Franke, M., Pytlak, Ł., Raaijmakers, C., Nowak, W., and Bodelier, P. L. E.: Methane-derived carbon as a driver for cyanobacterial growth, Front. Microbiol., 13, 1–16, https://doi.org/10.3389/fmicb.2022.837198, 2022.

Cicerone, R. J. and Oremland, R. S.: Biogeochemical aspects of atmospheric methane, Global Biogeochem. Cy., 2, 299–327, https://doi.org/10.1029/GB002i004p00299, 1988.

Collado-Fabbri, S., Vaulot, D., and Ulloa, O.: Structure and seasonal dynamics of the eukaryotic picophytoplankton community in a wind-driven coastal upwelling ecosystem, Limnol. Oceanogr., 56, 2334–2346, https://doi.org/10.4319/lo.2011.56.6.2334, 2011.

Cuevas, L. A., Daneri, G., Jacob, B., and Montero, P.: Microbial abundance and activity in the seasonal upwelling area off Concepción (∼ 36° S), central Chile: A comparison of upwelling and non-upwelling conditions, Deep-Sea Res. Pt. II, 51, 2427–2440, https://doi.org/10.1016/j.dsr2.2004.07.026, 2004.

Damm, E., Helmke, E., Thoms, S., Schauer, U., Nöthig, E., Bakker, K., and Kiene, R. P.: Methane production in aerobic oligotrophic surface water in the central Arctic Ocean, Biogeosciences, 7, 1099–1108, https://doi.org/10.5194/bg-7-1099-2010, 2010.

Damm, E., Beszczynska-Möller, T. A., Nöthing, E. M., and Kattner, G.: Methane excess production in oxygen-rich polar water and a model of cellular conditions for this paradox, Polar Sci., 9, 327–334, https://doi.org/10.1016/j.polar.2015.05.001, 2015.

De Angelis, M. A. and Lee, C.: Methane production during zooplankton grazing on marine phytoplankton, Limnol. Oceanogr., 39, 1298–1308, 1994.

De La Iglesia, R., Echenique-Subiabre, I., Rodríguez-Marconi, S., Espinoza, J. P., Von Dassow, P., Ulloa, O., and Trefault, N.: Distinct oxygen environments shape picoeukaryote assemblages thriving oxygen minimum zone waters off central Chile, J. Plankton Res., 42, 514–529, https://doi.org/10.1093/plankt/fbaa036, 2020.

Del Valle, D. A. and Karl, D. M.: Aerobic production of methane from dissolved water-column methylphosphonate and sinking particles in the North Pacific Subtropical Gyre, Aquat. Microb. Ecol., 73, 93–105, https://doi.org/10.3354/ame01714, 2014.

Dinasquet, J., Tiirola, M., and Azam, F.: Enrichment of bacterioplankton able to utilize one-carbon and methylated compounds in the Coastal Pacific Ocean, Front. Mar. Sci., 5, 1–13, https://doi.org/10.3389/fmars.2018.00307, 2018.

Dumestre, J. F., Guézennec, J., Galy-Lacaux, C., Delmas, R., Richard, S., and Labroue, L.: Influence of light intensity on methanotrophic bacterial activity in Petit Saut Reservoir, French Guiana, Appl. Environ. Microb., 65, 534–539, https://doi.org/10.1128/aem.65.2.534-539.1999, 1999.

Farías, L., Graco, M., and Ulloa, O.: Temporal variability of nitrogen cycling in continental-shelf sediments of the upwelling ecosystem off central Chile, Deep-Sea Res. Pt. II, 51, 2491–2505, https://doi.org/10.1016/j.dsr2.2004.07.029, 2004.

Farías, L., Fernández, C., Faúndez, J., Cornejo, M., and Alcaman, M. E.: Chemolithoautotrophic production mediating the cycling of the greenhouse gases N_2O and CH_4 in an upwelling ecosystem, Biogeosciences, 6, 3053–3069, https://doi.org/10.5194/bg-6-3053-2009, 2009.

Farías, L., Besoain, V., and García-Loyola, S.: Presence of nitrous oxide hotspots in the coastal upwelling area off central Chile: an analysis of temporal variability based on ten years of a biogeochemical time series, Environ. Res. Lett., 10, 1–13, https://doi.org/10.1088/1748-9326/10/4/044017, 2015.

Farías, L., Tenorio, S., Sanzana, K., and Faundez, J.: Temporal methane variability in the water column of an area of seasonal coastal upwelling: A study based on a 12 year time series, Prog. Oceanogr., 195, 102589, https://doi.org/10.1016/j.pocean.2021.102589, 2021.

Ferderlman, T. G., Lee, C., Pantoja, S., Harder, J., Bebout, B. M., and Fossing, H.: Sulfate reduction and methanogenesis in a *Thioploca*-dominates sediment off the coast of Chile, Geochim. Cosmochim. Ac., 61, 3065–3079, https://doi.org/10.1016/S0016-7037(97)00158-0, 1997.

Fernandez, C., González, M. L., Muñoz, C., Molina, V., and Farias, L.: Temporal and spatial variability of biological nitrogen fixation off the upwelling system of central Chile (35–38.5° S), J. Geophys. Res.-Oceans, 120, 3330–3349, https://doi.org/10.1002/2014JC010410, 2015.

Florez-Leiva, L., Damm, E., Farías, L., and Farias, L.: Methane production induced by dimethylsulfide in surface water of an upwelling ecosystem, Prog. Oceanogr., 112–113, 38–48, https://doi.org/10.1016/j.pocean.2013.03.005, 2013.

Gibb, S. W., Mantoura, R. F. C., Liss, P. S., and Barlow, R. G.: Distributions and biogeochemistries of methylamines and ammonium in the Arabian Sea, Deep-Sea Res. Pt. II, 46, 593–615, https://doi.org/10.1016/S0967-0645(98)00119-2, 1999.

Giovannoni, S. J., Delong, E. F., Schmidt, T. M., and Pace, N. R.: Tangential flow filtration and preliminary phylogenetic analysis of marine picoplankton, Appl. Environ. Microb., 56, 2572–2575, 1990.

Grasshoff, K., Ehrhardt, M., and Kremling, K.: Methods of Seawater Analysis, 2nd Edn., John Wiley & Sons, Ltd, Deerfield Beach, Florida, Verlag Chemie, 419 pp., https://doi.org/10.1002/iroh.19850700232, 1983.

Grossart, H. P., Frindte, K., Dziallas, C., Eckert, W., and Tang, K. W.: Microbial methane production in oxygenated water column of an oligotrophic lake, P. Natl. Acad. Sci. USA, 108, 19657–19661, https://doi.org/10.1073/pnas.1110716108, 2011.

Günthel, M., Donis, D., Kirillin, G., Ionescu, D., Bizic, M., McGinnis, D. F., Grossart, H. P., and Tang, K. W.: Contribution of oxic methane production to surface methane emission in lakes and its global importance, Nat. Commun., 10, 5497, https://doi.org/10.1038/s41467-019-13320-0, 2019.

Günthel, M., Klawonn, I., Woodhouse, J., Bižić, M., Ionescu, D., Ganzert, L., Kümmel, S., Nijenhuis, I., Zoccarato, L., Grossart, H. P., and Tang, K. W.: Photosynthesis-driven methane production in oxic lake water as an important contribu-

tor to methane emission, Limnol. Oceanogr., 65, 2853–2865, https://doi.org/10.1002/lno.11557, 2020.

Hahn, M. W.: Broad diversity of viable bacteria in "sterile" (0.2 µm) filtered water, Res. Microbiol., 155, 688–691, https://doi.org/10.1016/j.resmic.2004.05.003, 2004.

Hansell, D. A. and Orellana, M. V.: Dissolved organic matter in the global ocean: A primer, Gels, 7, 128, https://doi.org/10.3390/gels7030128, 2021.

Harmsen, M., van Vuuren, D. P., Bodirsky, B. L., Chateau, J., Durand-Lasserve, O., Drouet, L., Fricko, O., Fujimori, S., Gernaat, D. E. H. J., Hanaoka, T., Hilaire, J., Keramidas, K., Luderer, G., Moura, M. C. P., Sano, F., Smith, S. J., and Wada, K.: The role of methane in future climate strategies: mitigation potentials and climate impacts, Climatic Change, 163, 1409–1425, https://doi.org/10.1007/s10584-019-02437-2, 2020.

Hartmann, J. F., Günthel, M., Klintzsch, T., Kirillin, G., Grossart, H. P., Keppler, F., and Isenbeck-Schröter, M.: High spatiotemporal dynamics of methane production and emission in oxic surface water, Environ. Sci. Technol., 54, 1451–1463, https://doi.org/10.1021/acs.est.9b03182, 2020.

Holmes, E. M., Sansone, F. J., Rust, T. M., and Popp, B. N.: Methane production, consumption, and air-sea exchange in the open ocean: An evaluation based on carbon isotopic ratios, Global Biogeochem. Cy., 14, 1–10, https://doi.org/10.1029/1999GB001209, 2000.

Holm-Hansen, O., Lorenzen, C. J., Holmes, R. W., and Strickland, J. D. H.: Fluorometric determination of chlorophyll, Journal du Conseil International pour L'Exploration de la Mer, 30, 3–15, https://doi.org/10.1093/icesjms/30.1.3, 1965.

Igarza, M., Dittmar, T., Graco, M., and Niggemann, J.: Dissolved organic matter cycling in the coastal upwelling system off central Peru during an "El Niño" year, Front. Mar. Sci., 6, 1–17, https://doi.org/10.3389/fmars.2019.00198, 2019.

IPCC: Climate Change 2021 – The Physical Science Basis: Working Group I Contribution to the Sixth Assessment Report of the Intergovernmental Panel on Climate Change, Cambridge University Press, https://doi.org/10.1017/9781009157896, 2023.

Kara, A. B., Rochford, P. A., and Hurlburt, H. E.: Mixed layer depth variability over the global ocean, J. Geophys. Res.-Oceans, 108, 1–15, https://doi.org/10.1029/2000jc000736, 2003.

Karl, D. and Tilbrook, B.: Production and transport of methane in oceanic particulate organic matter, Nature, 368, 732–734, 1994.

Karl, D., Beversdorf, L., Björkman, K., Church, M., Martinez, A., and DeLong, E.: Aerobic production of methane in the sea, Nat. Geosci., 1, 473–478, https://doi.org/10.1038/ngeo234, 2008.

Klintzsch, T., Langer, G., Nehrke, G., Wieland, A., Lenhart, K., and Keppler, F.: Methane production by three widespread marine phytoplankton species: release rates, precursor compounds, and potential relevance for the environment, Biogeosciences, 16, 4129–4144, https://doi.org/10.5194/bg-16-4129-2019, 2019.

Klintzsch, T., Langer, G., Wieland, A., Geisinger, H., Lenhart, K., Nehrke, G., and Keppler, F.: Effects of temperature and light on methane production of widespread marine phytoplankton, J. Geophys. Res.-Biogeo., 125, 1–16, https://doi.org/10.1029/2020JG005793, 2020.

Klintzsch, T., Geisinger, H., Wieland, A., Langer, G., Nehrke, G., Bizic, M., Greule, M., Lenhart, K., Borsch, C., Schroll, M., and Keppler, F.: Stable carbon isotope signature of methane released from phytoplankton, Geophys. Res. Lett., 50, 1–12, https://doi.org/10.1029/2023gl103317, 2023.

Kock, A., Gebhardt, S., and Bange, H. W.: Methane emissions from the upwelling area off Mauritania (NW Africa), Biogeosciences, 5, 1119–1125, https://doi.org/10.5194/bg-5-1119-2008, 2008.

Lamontagne, R. A., Swinnerton, J. W., Linnenbom, V. J., and Smith, W. D.: Methane concentrations in various marine environments, J. Geophys. Res., 78, 5317–5324, https://doi.org/10.1029/JC078i024p05317, 1973.

Lenhart, K., Klintzsch, T., Langer, G., Nehrke, G., Bunge, M., Schnell, S., and Keppler, F.: Evidence for methane production by the marine algae *Emiliania huxleyi*, Biogeosciences, 13, 3163–3174, https://doi.org/10.5194/bg-13-3163-2016, 2016.

León-Palmero, E., Contreras-Ruiz, A., Sierra, A., Morales-Baquero, R., and Reche, I.: Dissolved CH_4 coupled to photosynthetic picoeukaryotes in oxic waters and to cumulative chlorophyll *a* in anoxic waters of reservoirs, Biogeosciences, 17, 3223–3245, https://doi.org/10.5194/bg-17-3223-2020, 2020.

Li, J. and Dittrich, M.: Dynamic polyphosphate metabolism in cyanobacteria responding to phosphorus availability, Environ. Microbiol., 21, 572–583, https://doi.org/10.1111/1462-2920.14488, 2019.

Li, Y., Fichot, C. G., Geng, L., Scarratt, M. G., and Xie, H.: The contribution of methane photoproduction to the oceanic methane paradox, Geophys. Res. Lett., 47, 1–10, https://doi.org/10.1029/2020GL088362, 2020.

Lidbury, I. D. E. A., Murrell, J. C., and Chen, Y.: Trimethylamine and trimethylamine N-oxide are supplementary energy sources for a marine heterotrophic bacterium: Implications for marine carbon and nitrogen cycling, ISME J., 9, 760–769, https://doi.org/10.1038/ismej.2014.149, 2015.

Llabrés, M., Agustí, S., and Herndl, G. J.: Diel in situ picophytoplankton cell death cycles coupled with cell division, J. Phycol., 47, 1247–1257, https://doi.org/10.1111/j.1529-8817.2011.01072.x, 2011.

Lohrer, C., Cwierz, P. P., Wirth, M. A., Schulz-Bull, D. E., and Kanwischer, M.: Methodological aspects of methylphosphonic acid analysis: Determination in river and coastal water samples, Talanta, 211, 1–8, https://doi.org/10.1016/j.talanta.2020.120724, 2020.

Lu, X., Jacob, D. J., Zhang, Y., Maasakkers, J. D., Sulprizio, M. P., Shen, L., Qu, Z., Scarpelli, T. R., Nesser, H., Yantosca, R. M., Sheng, J., Andrews, A., Parker, R. J., Boesch, H., Bloom, A. A., and Ma, S.: Global methane budget and trend, 2010–2017: complementarity of inverse analyses using in situ (GLOBALVIEWplus CH_4 ObsPack) and satellite (GOSAT) observations, Atmos. Chem. Phys., 21, 4637–4657, https://doi.org/10.5194/acp-21-4637-2021, 2021.

Ma, X., Sun, M., Lennartz, S. T., and Bange, H. W.: A decade of methane measurements at the Boknis Eck Time Series Station in Eckernförde Bay (southwestern Baltic Sea), Biogeosciences, 17, 3427–3438, https://doi.org/10.5194/bg-17-3427-2020, 2020.

Mao, S. H., Zhang, H. H., Zhuang, G. C., Li, X. J., Liu, Q., Zhou, Z., Wang, W. L., Li, C. Y., Lu, K. Y., Liu, X. T., Montgomery, A., Joye, S. B., Zhang, Y. Z., and Yang, G. P.: Aerobic oxidation of methane significantly reduces global diffusive methane emissions from shallow marine waters, Nat. Commun., 13, 7309, https://doi.org/10.1038/s41467-022-35082-y, 2022.

Martínez, A., Ventouras, L. A., Wilson, S. T., Karl, D. M., and DeLong, E. F.: Metatranscriptomic and functional metagenomic analysis of methylphosphonate utilization by marine bacteria, Front. Microbiol., 4, 340, https://doi.org/10.3389/fmicb.2013.00340, 2013.

McAuliffe, C.: Solubility in water of C1-C9 hydrocarbons, Nature, 200, 1092–1093, 1963.

McClain, M. E., Boyer, E. W., Dent, C. L., Gergel, S. E., Grimm, N. B., Groffman, P. M., Hart, S. C., Harvey, J. W., Johnston, C. A., Mayorga, E., McDowell, W. H., and Pinay, G.: Biogeochemical Hot Spots and Hot Moments at the Interface of Terrestrial and Aquatic Ecosystems, Ecosystems, 6, 301–312, https://doi.org/10.1007/s10021-003-0161-9, 2003.

Metcalf, W. W., Griffin, B. M., Cicchillo, R., Gao, J., Janga, S., Cooke, H., Circello, B., Evans, B., Martens-Habbena, W., Stahl, D., and Van Der Donk, W.: Synthesis of methylphosphonic acid by marine microbes: a source for methane in the Aerobic Ocean, Science, 337, 1104–1107, https://doi.org/10.1126/science.1219875, 2012.

Minor, E. C., Swenson, M. M., Mattson, B. M., and Oyler, A. R.: Structural characterization of dissolved organic matter: A review of current techniques for isolation and analysis, Environ. Sci.-Proc. Imp., 16, 2064–2079, https://doi.org/10.1039/c4em00062e, 2014.

Molina, V., Belmar, L., Levipan, H. A., Ramírez-Flandes, S., Anguita, C., Galán, A., Montes, I., and Ulloa, O.: Spatiotemporal distribution of key pelagic microbes in a seasonal oxygen-deficient coastal upwelling system of the Eastern South Pacific Ocean, Front. Mar. Sci., 7, 1–17, https://doi.org/10.3389/fmars.2020.561597, 2020.

Mopper, K., Kieber, D. J., and Stubbins, A.: Marine photochemistry of organic matter: processes and impacts. processes and impacts., in: Biogeochemistry of Marine Dissolved Organic Matter, edited by: Hansell, D. A. and Carlson, C. A., Elsevier Inc. Academic Press, 389–450, https://doi.org/10.1016/B978-0-12-405940-5.00008-X, 2015.

Morales, C. and Anabalón, V.: Phytoplankton biomass and microbial abundances during the spring upwelling season in the coastal area off Concepción, central-southern Chile: variability around a time series station, Prog. Oceanogr., 92–95, 81–91, https://doi.org/10.1016/j.pocean.2011.07.004, 2012.

Morales, C., González, H. E., Hormazabal, S. E., Yuras, G., Letelier, J., and Castro, L. R.: The distribution of chlorophyll-a and dominant planktonic components in the coastal transition zone off Concepción, central Chile, during different oceanographic conditions, Prog. Oceanogr., 75, 452–469, https://doi.org/10.1016/j.pocean.2007.08.026, 2007.

Morán, X. A. G., Estrada, M., Gasol, J. M., and Pedrós-Alió, C.: Dissolved primary production and the strength of phytoplankton-bacterioplankton coupling in contrasting marine regions, Microb. Ecol., 44, 217–223, https://doi.org/10.1007/s00248-002-1026-z, 2002.

Morana, C., Bouillon, S., Nolla-Ardèvol, V., Roland, F. A. E., Okello, W., Descy, J.-P., Nankabirwa, A., Nabafu, E., Springael, D., and Borges, A. V.: Methane paradox in tropical lakes? Sedimentary fluxes rather than pelagic production in oxic conditions sustain methanotrophy and emissions to the atmosphere, Biogeosciences, 17, 5209–5221, https://doi.org/10.5194/bg-17-5209-2020, 2020.

Muñoz-Marín, M. C., Gómez-Baena, G., López-Lozano, A., Moreno-Cabezuelo, J. A., Díez, J., and García-Fernández, J. M.: Mixotrophy in marine picocyanobacteria: use of organic compounds by *Prochlorococcus* and *Synechococcus*, ISME J., 14, 1065–1073, https://doi.org/10.1038/s41396-020-0603-9, 2020.

Oremland, R. S.: Methanogenic activity in plankton samples and fish intestines: A mechanism for in situ methanogenesis in oceanic surface waters, Limnol. Oceanogr., 24, 1136–1141, 1979.

Paul, L., Ferguson, D. J., and Krzycki, J. A.: The trimethylamine methyltransferase gene and multiple dimethylamine methyltransferase genes of methanosarcina barkeri contain in-frame and read-through amber codons, J. Bacteriol., 182, 2520–2529, 2000.

Rain-Franco, A., Sobarzo, M., Caparros, J., and Fernandez, C.: Variability of chromophoric dissolved organic matter in three freshwater-influenced systems along central-southern Chile, Prog. Oceanogr., 174, 154–161, https://doi.org/10.1016/j.pocean.2018.09.009, 2019.

Reeburgh, W. S.: Oceanic methane biogeochemistry, Chem. Rev., 107, 486–513, https://doi.org/10.1021/cr050362v, 2007.

Reintjes, G., Fuchs, B. M., Scharfe, M., Wiltshire, K. H., Amann, R., and Arnosti, C.: Short-term changes in polysaccharide utilization mechanisms of marine bacterioplankton during a spring phytoplankton bloom, Environ. Microbiol., 22, 1884–1900, https://doi.org/10.1111/1462-2920.14971, 2020.

Repeta, D. J., Ferrón, S., Sosa, O. A., Johnson, C. G., Repeta, L. D., Acker, M., DeLong, E. F., and Karl, D. M.: Marine methane paradox explained by bacterial degradation of dissolved organic matter, Nat. Geosci., 9, 1–7, https://doi.org/10.1038/ngeo2837, 2016.

Roth, F., Sun, X., Geibel, M. C., Prytherch, J., Brüchert, V., Bonaglia, S., Broman, E., Nascimento, F., Norkko, A., and Humborg, C.: High spatiotemporal variability of methane concentrations challenges estimates of emissions across vegetated coastal ecosystems, Glob. Change Biol., 28, 4308–4322, https://doi.org/10.1111/gcb.16177, 2022.

Saunois, M., Stavert, A. R., Poulter, B., Bousquet, P., Canadell, J. G., Jackson, R. B., Raymond, P. A., Dlugokencky, E. J., Houweling, S., Patra, P. K., Ciais, P., Arora, V. K., Bastviken, D., Bergamaschi, P., Blake, D. R., Brailsford, G., Bruhwiler, L., Carlson, K. M., Carrol, M., Castaldi, S., Chandra, N., Crevoisier, C., Crill, P. M., Covey, K., Curry, C. L., Etiope, G., Frankenberg, C., Gedney, N., Hegglin, M. I., Höglund-Isaksson, L., Hugelius, G., Ishizawa, M., Ito, A., Janssens-Maenhout, G., Jensen, K. M., Joos, F., Kleinen, T., Krummel, P. B., Langenfelds, R. L., Laruelle, G. G., Liu, L., Machida, T., Maksyutov, S., McDonald, K. C., McNorton, J., Miller, P. A., Melton, J. R., Morino, I., Müller, J., Murguia-Flores, F., Naik, V., Niwa, Y., Noce, S., O'Doherty, S., Parker, R. J., Peng, C., Peng, S., Peters, G. P., Prigent, C., Prinn, R., Ramonet, M., Regnier, P., Riley, W. J., Rosentreter, J. A., Segers, A., Simpson, I. J., Shi, H., Smith, S. J., Steele, L. P., Thornton, B. F., Tian, H., Tohjima, Y., Tubiello, F. N., Tsuruta, A., Viovy, N., Voulgarakis, A., Weber, T. S., van Weele, M., van der Werf, G. R., Weiss, R. F., Worthy, D., Wunch, D., Yin, Y., Yoshida, Y., Zhang, W., Zhang, Z., Zhao, Y., Zheng, B., Zhu, Q., Zhu, Q., and Zhuang, Q.: The Global Methane Budget 2000–2017, Earth Syst. Sci. Data, 12, 1561–1623, https://doi.org/10.5194/essd-12-1561-2020, 2020.

Schlitzer, R.: Ocean Data View, https://odv.awi.de (last access: 16 April 2024), 2023.

Schowanek, D. and Verstraete, W.: Phosphonate utilization by bacteria in the presence of alternative phosphorus sources, Biodegradation, Kluwer Academic Publishers, 1990 pp., https://doi.org/10.1007/BF00117050, 1990.

Sieburth, J., Smetacek, V., and Lenz, J.: Pelagic ecosystem structure: Heterotrophic compartments of the plankton and their relationship to plankton size fractions, Linmol. Oceanogr., 23, 1256–1263, https://doi.org/10.4319/lo.1978.23.6.1256, 1978.

Smith, M. W., Allen, L. Z., Allen, A. E., Herfort, L., and Simon, H. M.: Contrasting genomic properties of free-living and particle-attached microbial assemblages within a coastal ecosystem, Front. Microbiol., 4, 1–20, https://doi.org/10.3389/fmicb.2013.00120, 2013.

Sobarzo, M. and Djurfeldt, L.: Coastal upwelling process on a continental shelf limited by submarine canyons, Concepción, central Chile, J. Geophys. Res., 109, 1–20, https://doi.org/10.1029/2004JC002350, 2004.

Sobarzo, M., Bravo, L., Donoso, D., Garcés-Vargas, J., and Schneider, W.: Coastal upwelling and seasonal cycles that influence the water column over the continental shelf off central Chile, Prog. Oceanogr., 75, 363–382, https://doi.org/10.1016/j.pocean.2007.08.022, 2007.

Sosa, O. A., Repeta, D. J., DeLong, E. F., Ashkezari, M. D., and Karl, D. M.: Phosphate-limited ocean regions select for bacterial populations enriched in the carbon–phosphorus lyase pathway for phosphonate degradation, Environ. Microbiol., 21, 2402–2414, https://doi.org/10.1111/1462-2920.14628, 2019.

Sosa, O. A., Burrell, T. J., Wilson, S. T., Foreman, R. K., Karl, D. M., and Repeta, D. J.: Phosphonate cycling supports methane and ethylene supersaturation in the phosphate-depleted western North Atlantic Ocean, Limnol. Oceanogr., 65, 1–17, https://doi.org/10.1002/lno.11463, 2020.

Spilling, K., Camarena-Gómez, M. T., Lipsewers, T., Martinez-Varela, A., Díaz-Rosas, F., Eronen-Rasimus, E., Silva, N., von Dassow, P., and Montecino, V.: Impacts of reduced inorganic N : P ratio on three distinct plankton communities in the Humboldt upwelling system, Mar. Biol., 166, 1–17, https://doi.org/10.1007/s00227-019-3561-x, 2019.

Stefels, J. and Van Boekel, W.: Production of DMS from dissolved DMSP in axenic cultures of the marine phytoplankton species *Phaeocystis sp*, Mar. Ecol.-Prog. Ser., 97, 11–18, https://www.jstor.org/stable/24833593 (last access: 27 February 2024), 1993.

Strub, T., Mesías, J., Montecino, V., Rutllant, J., and Salinas, S.: Coastal ocean circulation off western south america, in: The global coastal ocean – regional studies and syntheses, vol. 11, edited by: Robinson, A. R. and Brink, K. H., John Wiley & Sons, Inc, NY, 273–313, 1998.

Sun, J., Steindler, L., Thrash, J. C., Halsey, K. H., Smith, D. P., Carter, A. E., Landry, Z. C., and Giovannoni, S. J.: One carbon metabolism in SAR11 pelagic marine bacteria, PLoS One, 6, 1–12, https://doi.org/10.1371/journal.pone.0023973, 2011.

Sun, J., Mausz, M. A., Chen, Y., and Giovannoni, S. J.: Microbial trimethylamine metabolism in marine environments, Environ. Microbiol., 21, 513–520, https://doi.org/10.1111/1462-2920.14461, 2019.

Taenzer, L., Carini, P. C., Masterson, A. M., Bourque, B., Gaube, J. H., and Leavitt, W. D.: Microbial Methane From Methylphosphonate Isotopically Records Source, Geophys. Res. Lett., 47, 1–9, https://doi.org/10.1029/2019GL085872, 2020.

Testa, G., Masotti, I., and Farías, L.: Temporal variability in net primary production in an upwelling area off central Chile (36° S), Front. Mar. Sci., 5, 1–17, https://doi.org/10.3389/fmars.2018.00179, 2018.

Upstill-Goddard, R. C. and Barnes, J.: Methane emissions from UK estuaries: Re-evaluating the estuarine source of tropospheric methane from Europe, Mar. Chem., 180, 14–23, https://doi.org/10.1016/j.marchem.2016.01.010, 2016.

Urata, S., Kurosawa, Y., Yamasaki, N., Yamamoto, H., Nishiwaki, N., Hongo, Y., Adachi, M., and Yamaguchi, H.: Utilization of phosphonic acid compounds by marine bacteria of the genera *Phaeobacter*, *Ruegeria*, and *Thalassospira* (α-Proteobacteria), FEMS Microbiol. Lett., 369, fnac065, https://doi.org/10.1093/femsle/fnac065, 2022.

Vargas, C. A., Martínez, R. A., Cuevas, L. A., Pavez, M. A., Cartes, C., González, H. E., Escribano, R., and Daneri, G.: The relative importance of microbial and classical food webs in a highly productive coastal upwelling area, Limnol. Oceanogr., 52, 1495–1510, https://doi.org/10.4319/lo.2007.52.4.1495, 2007.

Vargas, C. A., Arriagada, L., Sobarzo, M., Contreras, P. Y., and Saldías, G.: Bacterial production along a river-to-ocean continuum in central Chile: implications for organic matter cycling, Aquat. Microb. Ecol., 68, 195–213, https://doi.org/10.3354/ame01608, 2013.

Vargas, C. A., Contreras, P. Y., Pérez, C. A., Sobarzo, M., Saldías, G. S., and Salisbury, J.: Influences of riverine and upwelling waters on the coastal carbonate system off Central Chile and their ocean acidification implications, J. Geophys. Res.-Biogeo., 121, 1–16, https://doi.org/10.1002/2015JG003213, 2016.

Wang, Q., Dore, J. E., and McDermott, T. R.: Methylphosphonate metabolism by *Pseudomonas sp.* populations contributes to the methane oversaturation paradox in an oxic freshwater lake, Environ. Microbiol., 19, 1–41, https://doi.org/10.1111/1462-2920.13747, 2018.

Wang, Q., Alowaifeer, A., Kerner, P., Balasubramanian, N., Patterson, A., Christian, W., Tarver, A., Dore, J. E., Hatzenpichler, R., Bothner, B., and McDermott, T. R.: Aerobic bacterial methane synthesis, P. Natl. Acad. Sci. USA, 118, 1–9, https://doi.org/10.1073/pnas.2019229118, 2021.

Wanninkhof, R.: Relationship between wind speed and gas exchange over the ocean, J. Geophys. Res., 97, 7373–7382, https://doi.org/10.1029/92JC00188, 1992.

Weber, T., Wiseman, N. A., and Kock, A.: Global ocean methane emissions dominated by shallow coastal waters, Nat. Commun., 10, 1–10, https://doi.org/10.1038/s41467-019-12541-7, 2019.

Wiesenburg, D. A. and Guinasso, N. L.: Equilibrium solubilities of methane, carbon monoxide, and hydrogen in water and sea water, American Chemical Society, 24, 356–360, 1979.

Worden, A.: Picoeukaryote diversity in coastal waters of the Pacific Ocean, Aquat. Microb. Ecol., 43, 165–175, https://doi.org/10.3354/ame043165, 2006.

Xu, S., Sun, Z., Geng, W., Cao, H., Zhang, X., Zhai, B., and Wu, Z.: Advance in Numerical Simulation Research of Marine Methane Processes, Front. Earth Sci., 10, 891393, https://doi.org/10.3389/feart.2022.891393, 2022.

Ye, W. W., Wang, X. L., Zhang, X.-H., and Zhang, G.-L.: Methane production in oxic seawater of the western North Pacific and its marginal seas, Limnol. Oceanogr., 65, 1–14, https://doi.org/10.1002/lno.11457, 2020.

Zhang, Y. and Xie, H.: Photomineralization and photomethanification of dissolved organic matter in Saguenay River surface water, Biogeosciences, 12, 6823–6836, https://doi.org/10.5194/bg-12-6823-2015, 2015.

Zhao, L., Lin, L.-Z., Chen, M.-Y., Teng, W.-K., Zheng, L.-L., Peng, L., Lv, J., Brand, J. J., Hu, C.-X., Han, B.-P., Song, L.-R., and Shu, W.-S.: The widespread capability of methylphosphonate utilization in filamentous cyanobacteria and its ecological significance, Water Res., 217, 1–11, https://doi.org/10.1016/j.watres.2022.118385, 2022.